AD

USAAVLABS TECHNICAL REPORT 69-30

EFFECT OF FIBER DIRECTION ON THE INSTABILITY OF SINGLE-LAYER GLASS-CLOTH RESIN-IMPREGNATED CYLINDERS UNDER UNIFORM AXIAL COMPRESSION

By

Joseph John Minecci

September 1971

EUSTIS DIRECTORATE
U. S. ARMY AIR MOBILITY RESEARCH AND DEVELOPMENT LABORATORY
FORT EUSTIS, VIRGINIA

CONTRACT DA 44-177-AMC-115(T)
STANFORD UNIVERSITY
STANFORD, CALIFORNIA

DEPARTMENT OF THE ARMY
U. S. ARMY AIR MOBILITY RESEARCH & DEVELOPMENT LABORATORY
EUSTIS DIRECTORATE
FORT EUSTIS, VIRGINIA 23604

This program was conducted under Contract DA 44-177-AMC-115(T) with Stanford University, Stanford, California.

The data contained in this report are the result of research to determine whether fiber direction would influence the stability level of a thin-walled circular cylindrical shell under uniform axial compression. Single-layer glass-epoxy shells were studied, varying fiber direction with the loading axis. The effect of repeated loading is also presented.

The report has been reviewed by this Directorate and is considered to be technically sound. It is published for the exchange of information and the stimulation of future research.

This program was conducted under the technical management of Mr. James P. Waller, Structures Division

DISCLAIMER

The findings in this report are not to be construed as an official Department of the Army position unless so designated by other authorized documents.

When Government drawings, specifications, or other data are used for any purpose other than in connection with a definitely related Government procurement operation, the United States Government thereby incurs no responsibility nor any obligation whatsoever; and the fact that the Government may have formulated, furnished, or in any way supplied the said drawings, specifications, or other data is not to be regarded by implication or otherwise as in any manner licensing the holder or any other person or corporation, or conveying any rights or permission, to manufacture, use, or sell any patented invention that may in any way be related thereto.

Trade names cited in this report do not constitute an official endorsement or approval of the use of such commercial hardware or software.

DISPOSITION INSTRUCTIONS

Destroy this report when no longer needed. Do not return it to the originator.

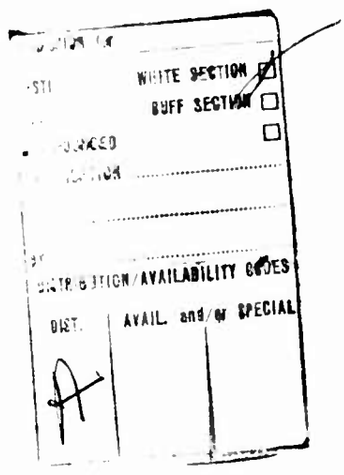

Task 1F162204A17002
Contract DA 44-177-AMC-115(T)
USAAVLABS Technical Report 69-30
September 1971

EFFECT OF FIBER DIRECTION ON THE INSTABILITY OF SINGLE-LAYER GLASS-CLOTH RESIN-IMPREGNATED CYLINDERS UNDER UNIFORM AXIAL COMPRESSION

By

Joseph John Minecci

Prepared by

Stanford University
Stanford, California

for

EUSTIS DIRECTORATE
U.S. ARMY AIR MOBILITY RESEARCH AND DEVELOPMENT LABORATORY
FORT EUSTIS, VIRGINIA

Unclassified

Security Classification

DOCUMENT CONTROL DATA - R & D

(Security classification of title, body of abstract and indexing annotation must be entered when the overall report is classified)

1. ORIGINATING ACTIVITY (Corporate author) Stanford University Stanford, Calif.	2a. REPORT SECURITY CLASSIFICATION Unclassified 2b. GROUP

3. REPORT TITLE

EFFECT OF FIBER DIRECTION ON THE INSTABILITY OF SINGLE-LAYER GLASS-CLOTH RESIN-IMPREGNATED CYLINDERS UNDER UNIFORM AXIAL COMPRESSION

4. DESCRIPTIVE NOTES (Type of report and inclusive dates)

5. AUTHOR(S) (First name, middle initial, last name)

Minecci, Joseph John

6. REPORT DATE	7a. TOTAL NO. OF PAGES	7b. NO. OF REFS
September 1971	61	15

8a. CONTRACT OR GRANT NO	9a. ORIGINATOR'S REPORT NUMBER(S)
DA 44-177-AMC-115(T) b. PROJECT NO. Task 1F162204A17002 c. d.	USAAVLABS Technical Report 69-30 9b. OTHER REPORT NO(S) (Any other numbers that may be assigned this report)

10. DISTRIBUTION STATEMENT

Approved for public release; distribution unlimited.

11. SUPPLEMENTARY NOTES	12. SPONSORING MILITARY ACTIVITY
	Eustis Directorate, U.S. Army Air Mobility Research and Development Laboratory, Fort Eustis, Virginia

13. ABSTRACT

This report presents the results of a series of experiments made on the effect of fiber direction on the compressive strength, stability, and stiffness of single-layer glass-cloth resin impregnated cylinders. It shows that while such direction is of extreme importance to the issues of strength and stiffness it does not significantly influence the critical load magnitudes. It demonstrates further that under repeated loading increasing damage is experienced by the fibers as their direction becomes more skew to the fold lines.

DD FORM 1 NOV 68 1473

Unclassified

Security Classification

SUMMARY

The effect of fiber direction on the instability of single-layer glass-cloth resin-impregnated cylinders under uniform axial compression was studied. 108 cylinders in subgroups in which the fiber directions were at 0°, 30°, 45°, and 90° to the principal "directions" of the shell were used in the investigation. These were tested in a standard Baldwin 60,000-pound universal test machine. End shortening was measured by dial gages and the load was applied at a constant but reasonably low rate. The results were statistically analyzed, and they indicate that while fiber direction is of extreme importance in questions of strength or stiffness it does not naturally influence the initial critical loads.

Unclassified
Security Classification

14 KEY WORDS	LINK A		LINK B		LINK C	
	ROLE	WT	ROLE	WT	ROLE	WT
Stability						
Strength						
Stiffness						
Fiber cylinders						
Direction of Fibers, effect						

Unclassified
Security Classification

8951-71

FOREWORD

The research described herein is part of a general investigation of composite structures being carried out by the Department of Aeronautics and Astronautics at Stanford University and is sponsored by the U. S. Army Aviation Materiel Laboratories under Contract DA 44-177-AMC-115(T)(task 1F162204A17002).

BLANK PAGE

TABLE OF CONTENTS

LIST OF ILLUSTRATIONS

LIST OF TABLES

LIST OF SYMBOLS

α	a number such that $100(1 - \alpha)$ is the percent probability of acceptance when true
β	a number such that $100(1 - \beta)$ is the percent probability of acceptance when false
μ_o	grand mean of all load values
σ	standard deviation of load values
d	detectable error/2 standard deviations
g	test statistic for Cochran's test
K	number of variances
n	sample size
n_x	number of degrees of freedom for load
n_y	number of degrees of freedom for angle
$\bar{x}$	mean value of individual angles
x_1	individual values of load
y_1	individual values of angle

INTRODUCTION

Shell bodies find general application in engineering. The behavior of such structures under a wide variety of load conditions has therefore been the subject of much research, both theoretical and experimental. According to Nash [1,2] some 2,339 books and papers were published on the subject prior to 1956. Many more have been published since. Perhaps the most commonly investigated problem, and certainly one of the most perplexing, is the stability of circular cylindrical shells subjected to axial compressive forces.[3] No correlation exists between theoretical predictions and observed behaviors.[4] There is, without doubt, a need for a clearer insight into the fundamental mechanism of the buckling process.[5] Present-day experimental researches are directed toward this understanding.[6]

The problems of nonuniform load distribution, such as are encountered in cylindrical shells under bending or bending in association with direct load, are just as complex and just as unpredictable. Recent experimental studies[7] show that under these conditions, there is a 1:1 correspondence between buckle shapes and critical stresses for the cases of flexure and direct load.

The history of engineering shows that pioneering structures have been designed, built, and successfully used without the aid of theory. But, there has always been concentrated research to rectify this unsatisfactory situation. So it is today. Progress in materials development has been very marked within the last two decades. Fibers with extremely good basic properties have been developed. Notable examples are those of glass, boron, and carbon. The basic properties of these materials are found in Figures 1 through 4[8], where they are compared with common metals.

Engineers have been quick to realize the potential of these materials, and structures fabricated from fiber elements in resin matrices are now finding much application. Filament-wound motor cases have been used in several weapon systems, and studies have been made to evaluate the feasibility of a counterinsurgency aircraft fabricated from glass-cloth laminates.[9] However, in these developments there are two fundamental problems. First, there is a lack of satisfactory data on mechanical properties. Second, satisfactory analytical predictions of the strength of thin shell bodies cannot be made. This latter area presents two challenges: reliability must be achieved, and the nonisotropic nature of the material must be accounted for.

The present research was undertaken as part of a program of experimental and analytical study of fiber composite structures. Its aim was to determine whether or not fiber direction would influence the stability level, as distinct from the strength, of a thin-walled circular cylindrical shell under uniform axial compression.

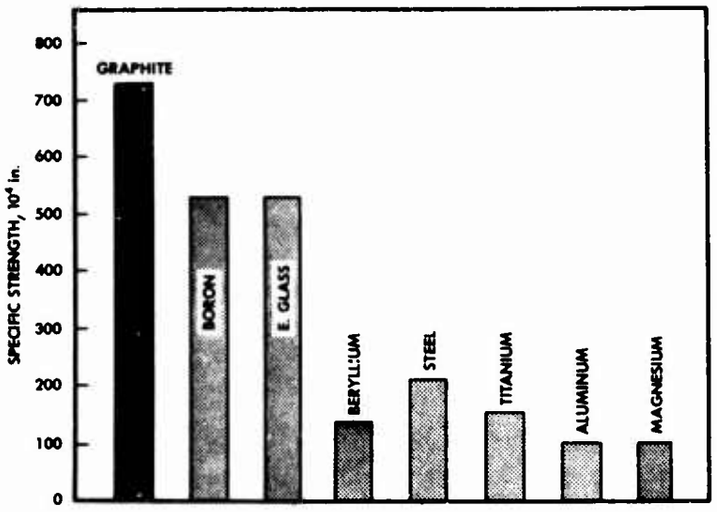

Figure 1. Strength-Weight Ratios for Various Materials.

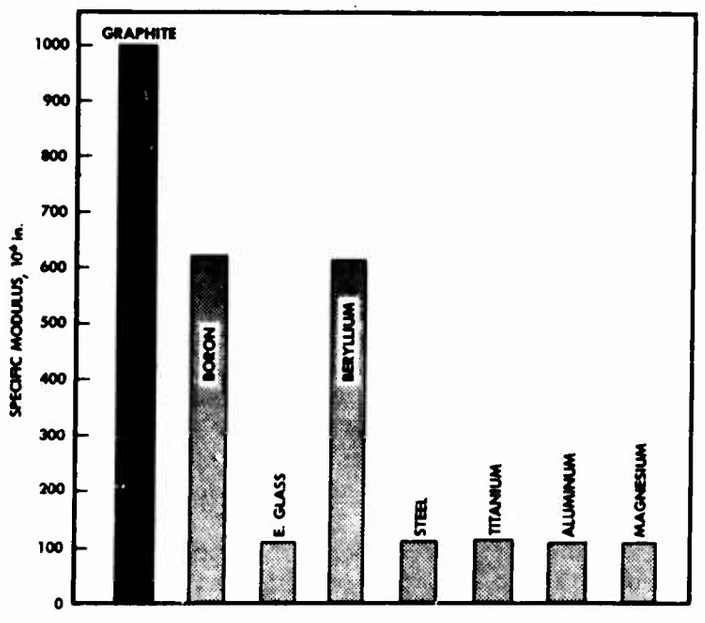

Figure 2. Stiffness-Weight Ratios for Various Materials.

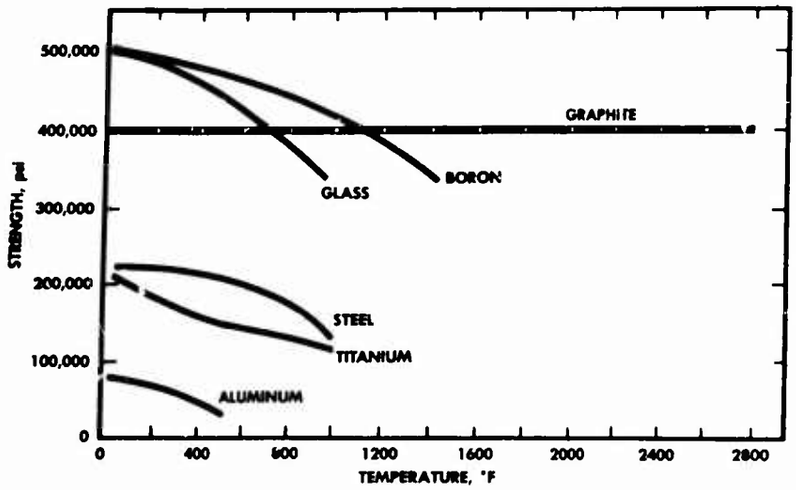

Figure 3. Strength vs. Temperature for Various Materials.

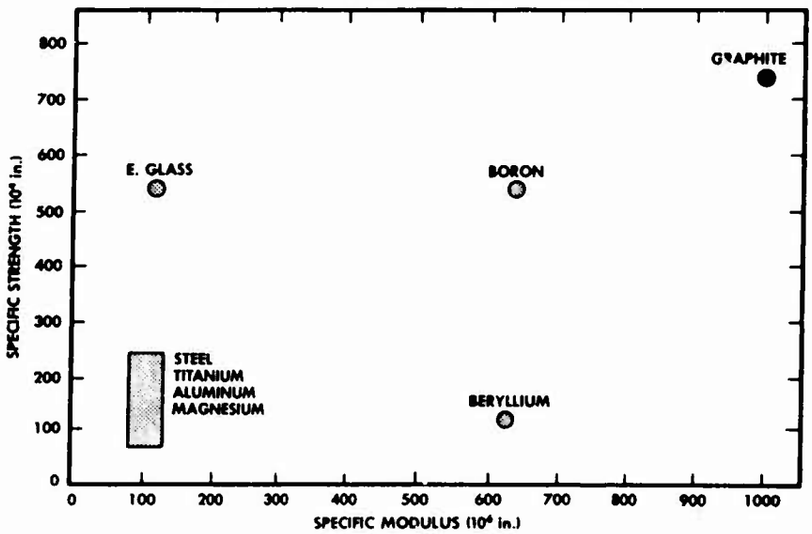

Figure 4. Specific Strength vs. Specific Modulus for Various Materials.

DISCUSSION OF THE PROBLEM

Very few theoretical or experimental studies have been made for heterogeneous aeolotropic bodies. Admittedly, Cheng and Ho[10] have published a small deflection treatment of the stability of heterogeneous aeolotropic cylindrical shells under combined loading, and Ho and Cheng[11] have compared this work with limited test data. However, these authors have emphasized in their work that axial load should be limited to tension or small compression in combination with other loads. This remark is most pertinent, since similar theoretical treatments do not agree with experiment even in the case of isotropic materials. It must be pointed out that the theory of Cheng and Ho, although applicable to heterogeneous anisotropic materials, is based on the classical Kirchoff-Love assumption for the preservation of normal fibers during deformation. That such an assumption is valid in the buckling problem of heterogeneous anisotropic materials of the fiber-reinforced matrix type has not been established.

Experience tells us that knowledge is developed by studying the simplest model under the simplest circumstance and by progression from this state to the more complex. Thus, there would seem to be a profitable area of experimental study in the single-layer glass-cloth resin-impregnated cylindrical shell under uniform axial compression. The simplest question which can be posed is, does fiber direction significantly influence the critical compressive load for such a body?

OUTLINE OF THE RESEARCH PROGRAM

Within the present framework of knowledge, the apparently simple question of the preceding section is extremely difficult to answer by analytical means. Thus, it was decided to study the problem experimentally. The problem, then, is to construct a family of shells of nominally identical exterior geometry with various internal geometrical arrangements of fiber and to test these specimens under closely controlled conditions. In the interest of simplicity, the shell chosen for this study was to be made from a single layer of resin-impregnated glass-cloth. Four arrangements of fiber were chosen, and some 25 specimens in each class were desired.

DESCRIPTION OF SPECIMENS

The cylindrical shells used for the first series of tests had an OD of 4-7/8 inches and were approximately 10 inches long. The maximum out-of-roundness was of the order of 2 percent of the diameter, and the maximum taper was of the same order. The material from which they were made was an open-weave glass cloth woven from E-Volan A glass fiber, stabilized by a resin system. The cloth had 18 fibers per inch in the warp direction and 16 in the fill direction, and it was classified by the maker as "Boatcloth". The resin used was Epon 827, and the hardener was diethylenetriamine; the system consisted of 100 parts resin to 11 parts hardener.

The open-weave cloth was chosen for two reasons: first, it should tend to magnify the variations due to angle of weave; second, the precise determination of angle should be relatively simple optically. Thus, the rejection of specimens in which marked local deviations of fiber direction existed should be an easy matter.

MANUFACTURE OF SPECIMENS

Appropriate lengths of cloth were freed from wrinkles, aligned, and impregnated with resin in as uniform a manner as possible while in contact with a warm Teflon-coated aluminum plate. The material prepared in this manner was then partially cured at 150°F for 15 minutes. After this treatment, the material was easy to handle, and blanks of appropriate size and directional property were sheared out. The rectangular elements so produced were next inserted into a circular cylindrical manufacturing oven, in which they were simultaneously spun and heated. The spinning forced the material into a cylindrical shape, and the heating completed the curing process.

Heat was provided by quartz tubular heaters, mounted inside the oven and positioned on the horizontal diameter, being symmetrical about the axis of rotation. These elements have a rated output of 1000 watts at 240 volts, but they were operated at 120 volts. They were used for 30 minutes of the forming cycle, and in this time they raised the specimen temperature to a maximum value of 250°F. During the heating phase of the curing cycle, the rotational speed was 230 rpm. This phase was followed by 30 minutes of natural cooling, during which the speed was increased to 460 rpm.

The cured specimens were circular cylindrical forms free of locked-in stresses, since the maximum curing temperature was in excess of the heat distortion temperature for the resin system.

To keep the seam in the shell from being appreciably stronger or stiffer than that in the main body, the bond was made with Duco cement. The fact that the buckle pattern frequently included the seam section may be cited as evidence that this state was achieved.

The final process in specimen preparation was to trim the ends by means of a hand-held cutting wheel. By spinning the vehicle during this operation, the ends were cut square to within 1/32 inch.

The manufacturing stages and equipment are shown in Figures 5a through 5f.

a. Resin-Impregnated Material.

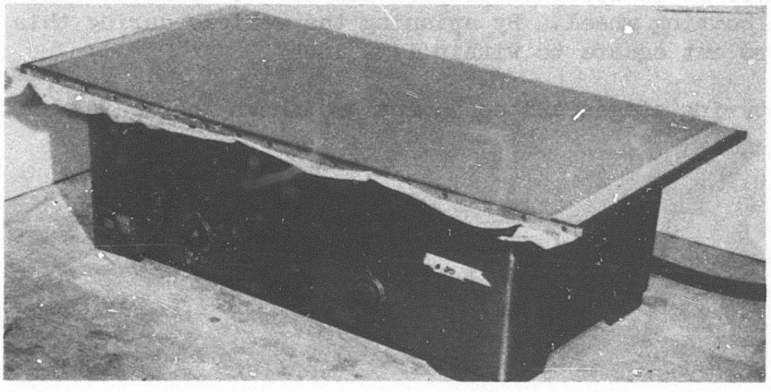

b. Initial Curing.

Figure 5. Manufacture of Specimens.

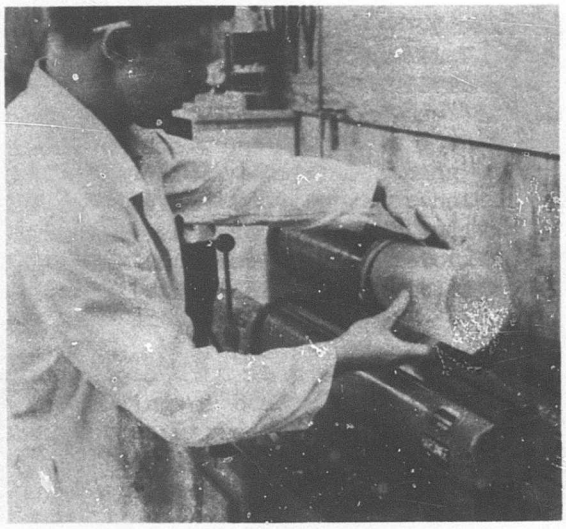

c. Inserting Blanks in Curing Oven.

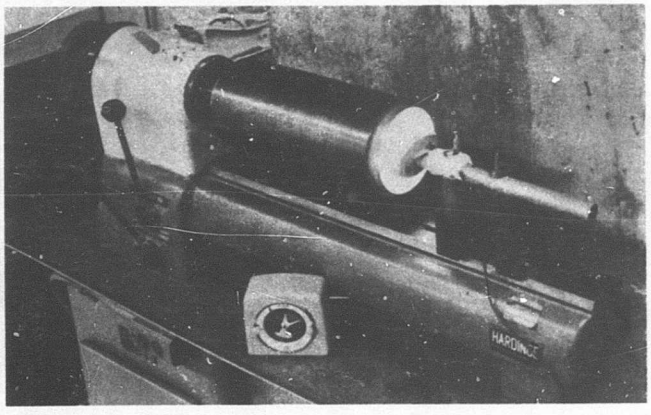

d. Curing Oven in Operation.

Figure 5. Continued.

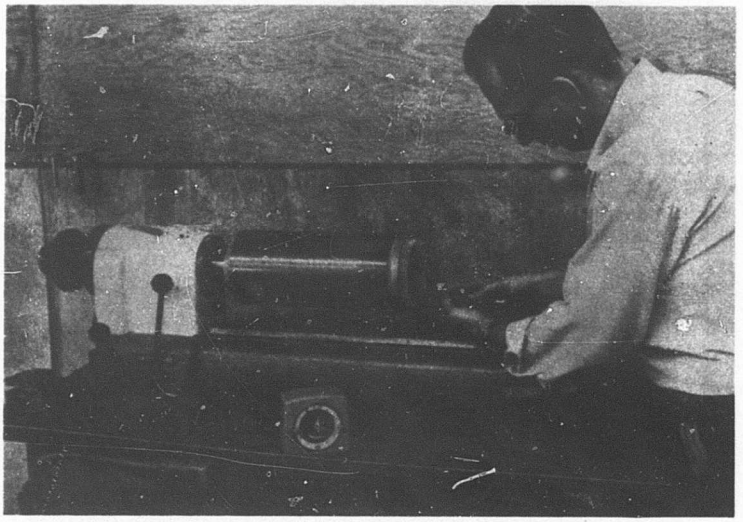

e. Trimming the Ends.

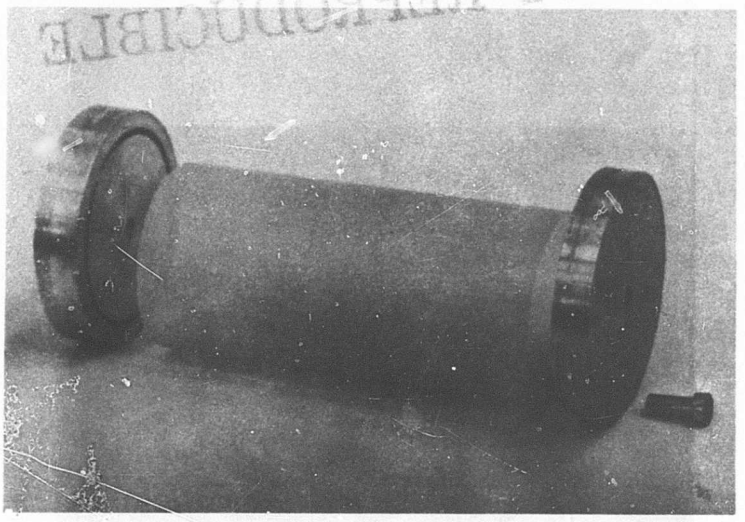

f. The Completed Specimen, With End Plates, Prior to Installation.

Figure 5. Continued.

SPECIMEN PREPARATION FOR INSPECTION AND TEST

The specimens, fabricated as described in the preceding section, were mounted in end plates. These plates, shown in Figure 6, consisted of an aluminum alloy disc in which a circular groove 1/8-inch wide and 1/4-inch deep was cut to house the specimen ends. Concentric with this groove, a 1/2-inch hole was drilled and reamed to accept multipurpose high-accuracy plugs. For quality control, identical plugs with machined centers were inserted in each end, and the specimen was mounted between centers and was viewed in the optical comparator, as described in the next section. For test purposes, the upper insert was drilled to receive a spherical bearing, while the lower insert was used as an alighment fixture to ensure concentricity with the load cell beneath.

Consistency of end conditions was assured by casting the ends into the circular groove in the end plates. The casting medium, chosen for its rapid curing properties, was an epoxy resin system consisting of Epon 828 plus 24 parts per hundred of curing agent T-1. A silicone parting agent was used in the groove to facilitate removal of the specimens after test. The casting can be seen clearly in Figure 7, which shows a specimen partially removed from the end plates after testing. A fully mounted cylinder is shown in Figure 8.

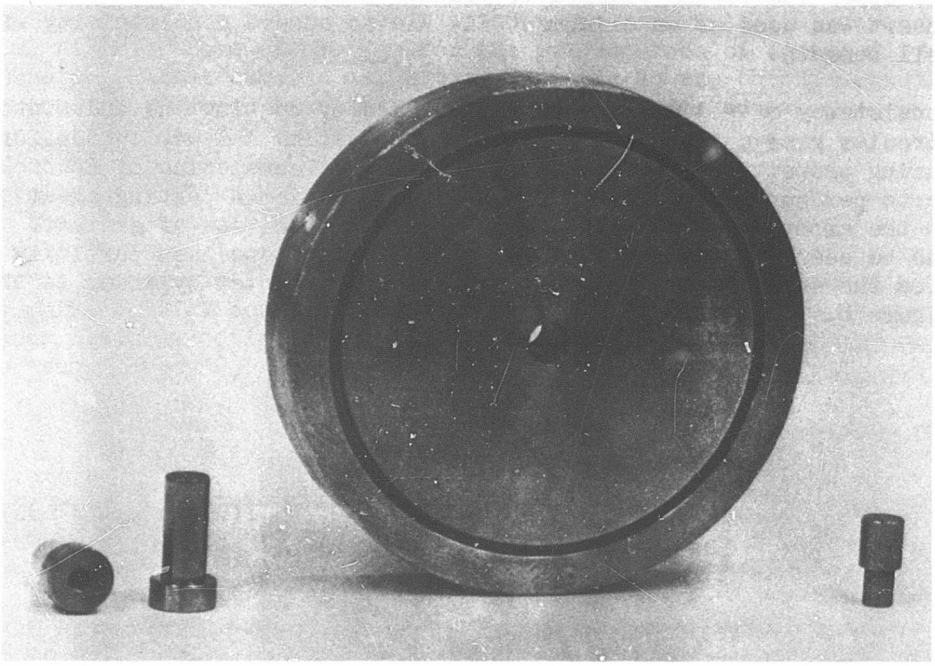

Figure 6. View of End Plate With Inserts.

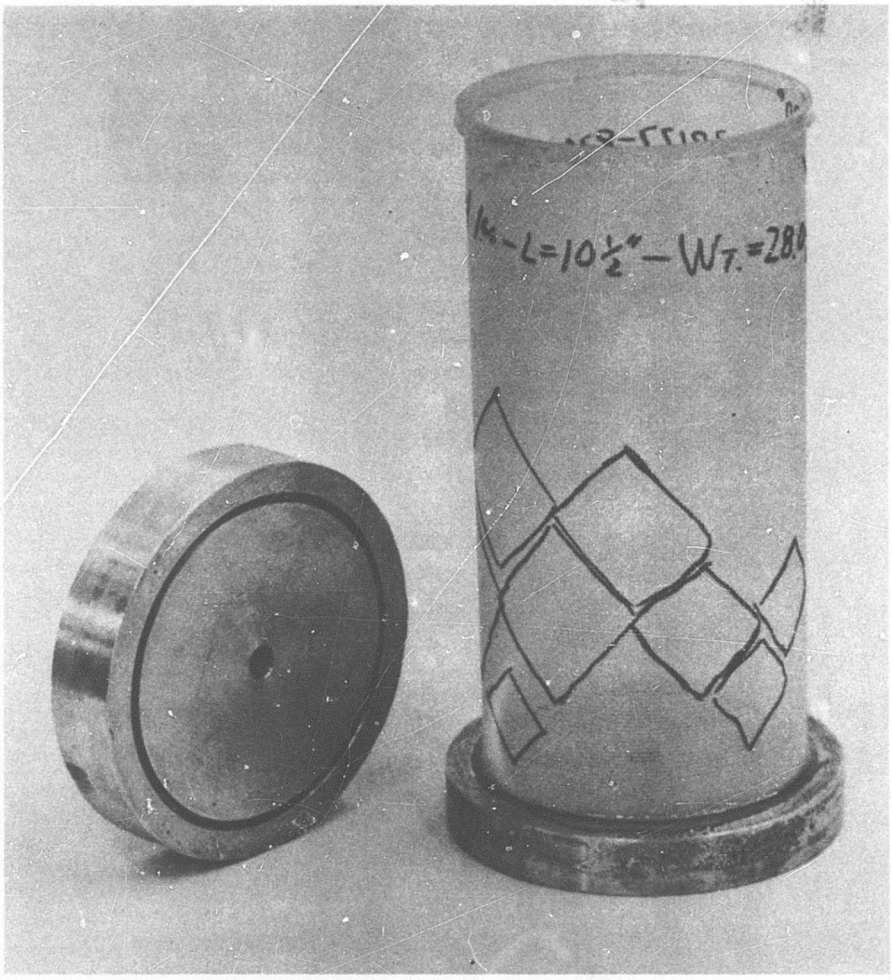

Figure 7. Cylinder After Removal From End Plates.

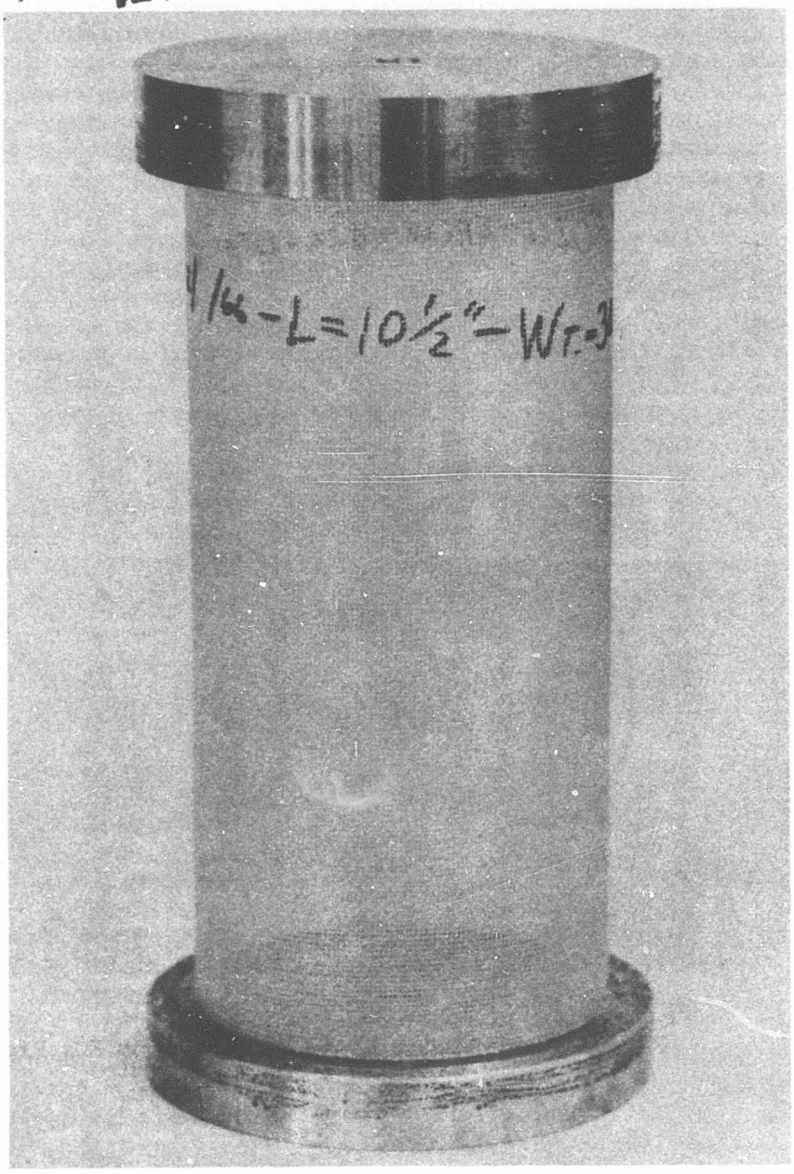

Figure 8. Fully Mounted Cylinder.

INSPECTION PROCEDURE

Each of the test specimens was inspected twice. At the first inspection the specimens were weighed, dimensionally checked, and visually inspected for adequate seaming. The second inspection was made after the specimens were installed in the end plates. Appropriate plugs were fitted into these plates, and the shell-plate system was mounted between centers in a special fixture. This fixture was carefully aligned on the table of a Bausch and Lomb optical comparator, shown in Figure 9. The light passed through the lower portion of the shell, and the uppermost surface was brought into focus. The magnified image of a local region of the shell, clearly depicted in Figures 9 and 10, enabled local fiber quality and direction to be determined. Checks of this kind were made at 20 randomly located regions on the surface of the specimen. Additionally, the comparator was used to ensure that all vehicles passed through to the test stage not only had satisfactory weave angles but also were straight-sided and reasonably circular.

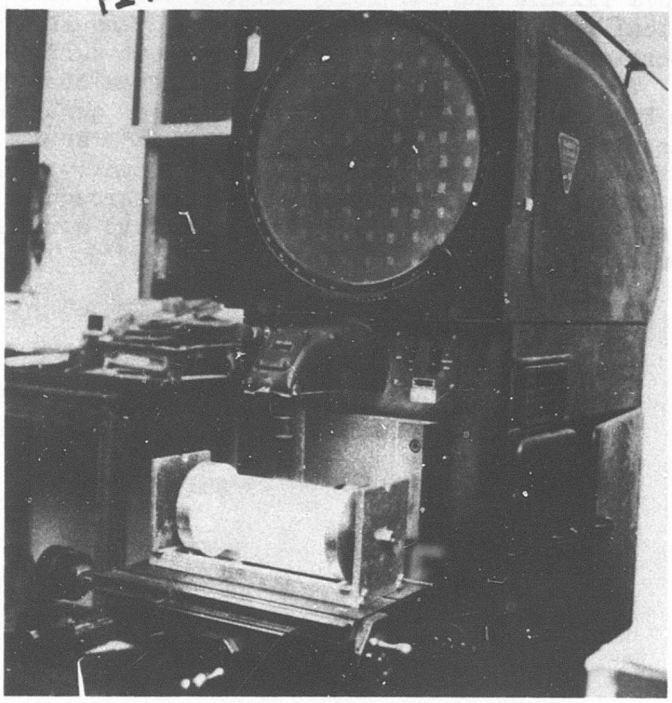

Figure 9. Overall View of Comparator, With Cylinder Mounted for Observation.

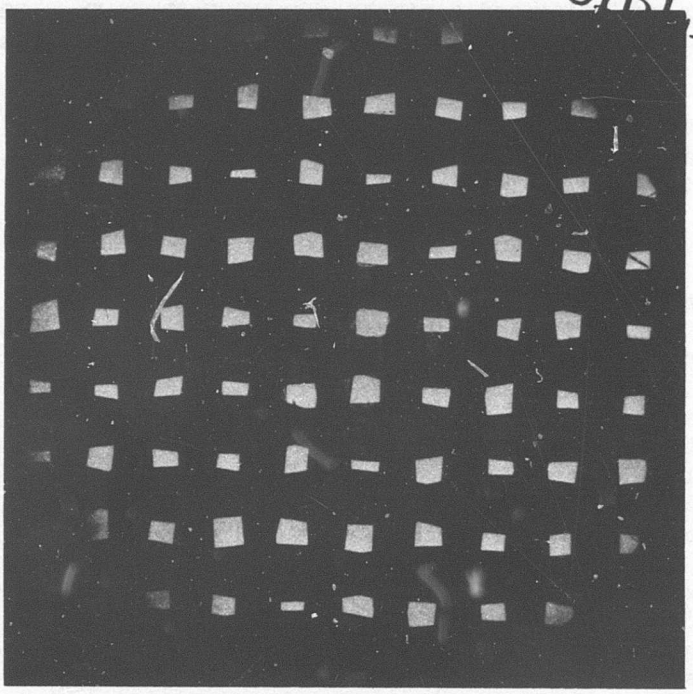

Figure 10. Comparator Screen, Showing Upper Surface of Cylinder, Magnified 32.5 Times.

TEST PROCEDURE AND INSTRUMENTATION

All tests were made in a standard Baldwin-Southwark 60,000-pound-capacity universal test machine. Since the load levels anticipated were small and since an accurate value of load drop-off was desired, the loadings were determined from a strain-gage proving ring. This ring was gaged with Baldwin SR-4 wire gages and was used in conjunction with a Model 1500 Sanborn carrier amplifier and a single-channel Sanborn Type 300 pen recorder. With this arrangement, load values could be determined to an accuracy of ± 2 pounds.

Axiality of load was assured by careful alignment of the axis of the load cell and the test vehicle and by applying the force to the specimen via a spherical bearing accurately located on the centerline of the system. End shortening was measured by means of a 1/1,000-inch dial gage. The test arrangement is shown in Figures 11 through 14.

Load was applied at a constant rate until buckling occurred. At this point, the load level was held steady at the drop-off value while the buckle pattern was observed and sketched on the surface of the shell.

The rate of load application was kept low in order that end-shortening readings could be taken from the 1/1,000-inch dial gage. These readings were recorded manually. Correlation of load and displacement readings was made by impressing a time mark on the load reading record. This marker was actuated by a contact switch which was pressed as the reading was taken.

A second test was made on each shell. The procedure followed was the same as that used for the first test except that no end shortenings were recorded. This repetition provided a check on repeatability, as well as evaluation of the damage caused on the first run.

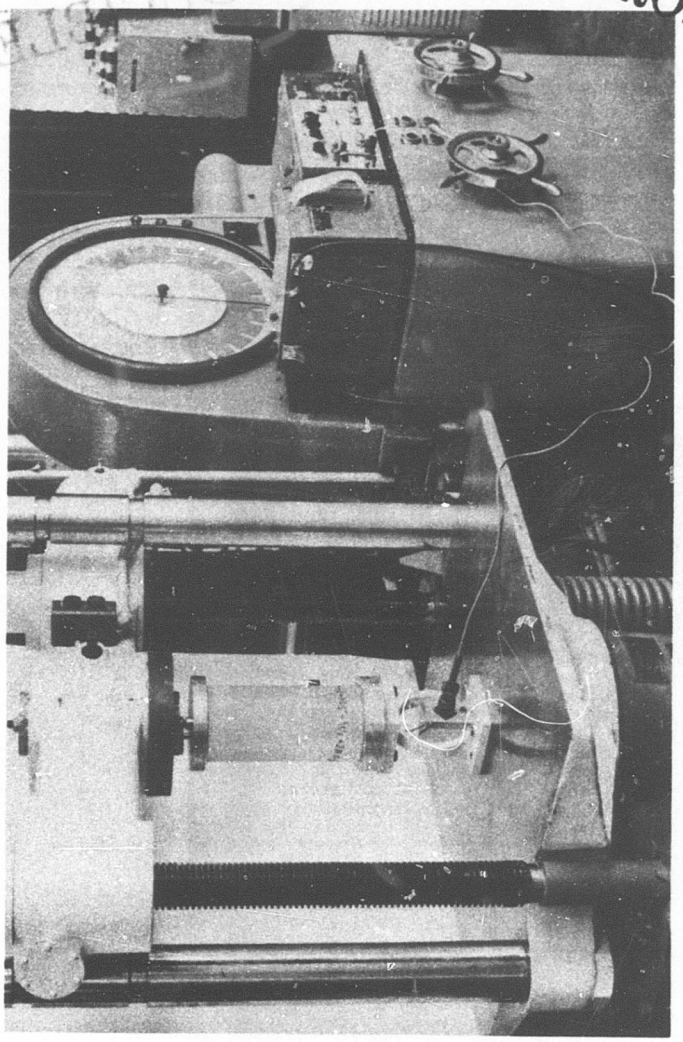

Figure 11. Overall View of Test Machine.

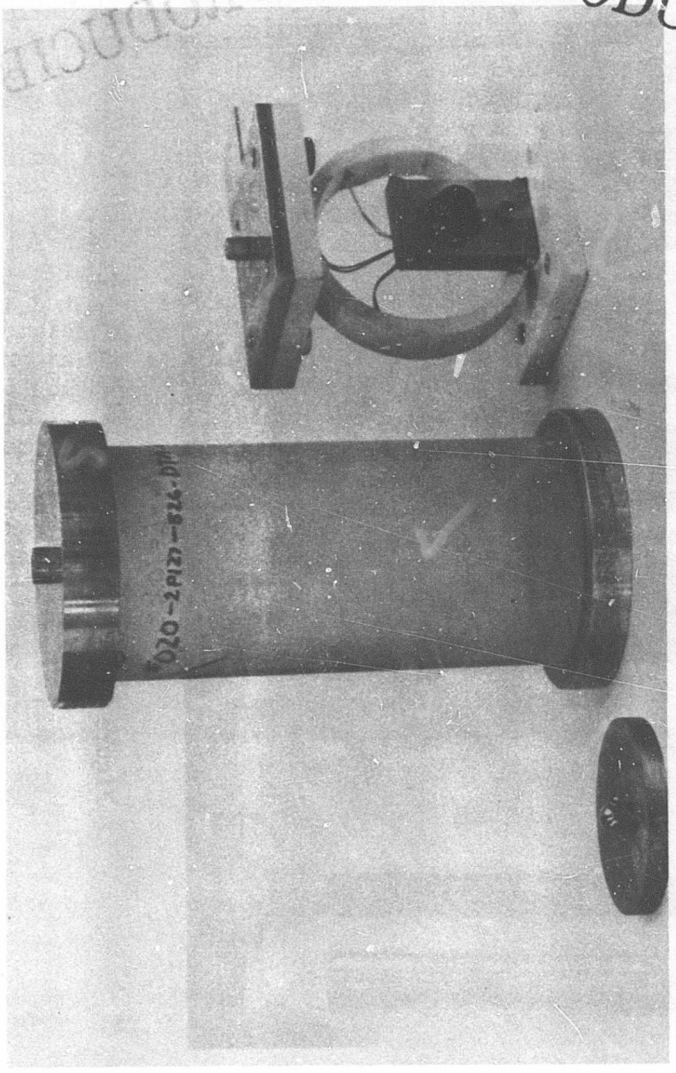

Figure 12. Component Parts of the Test Rig.

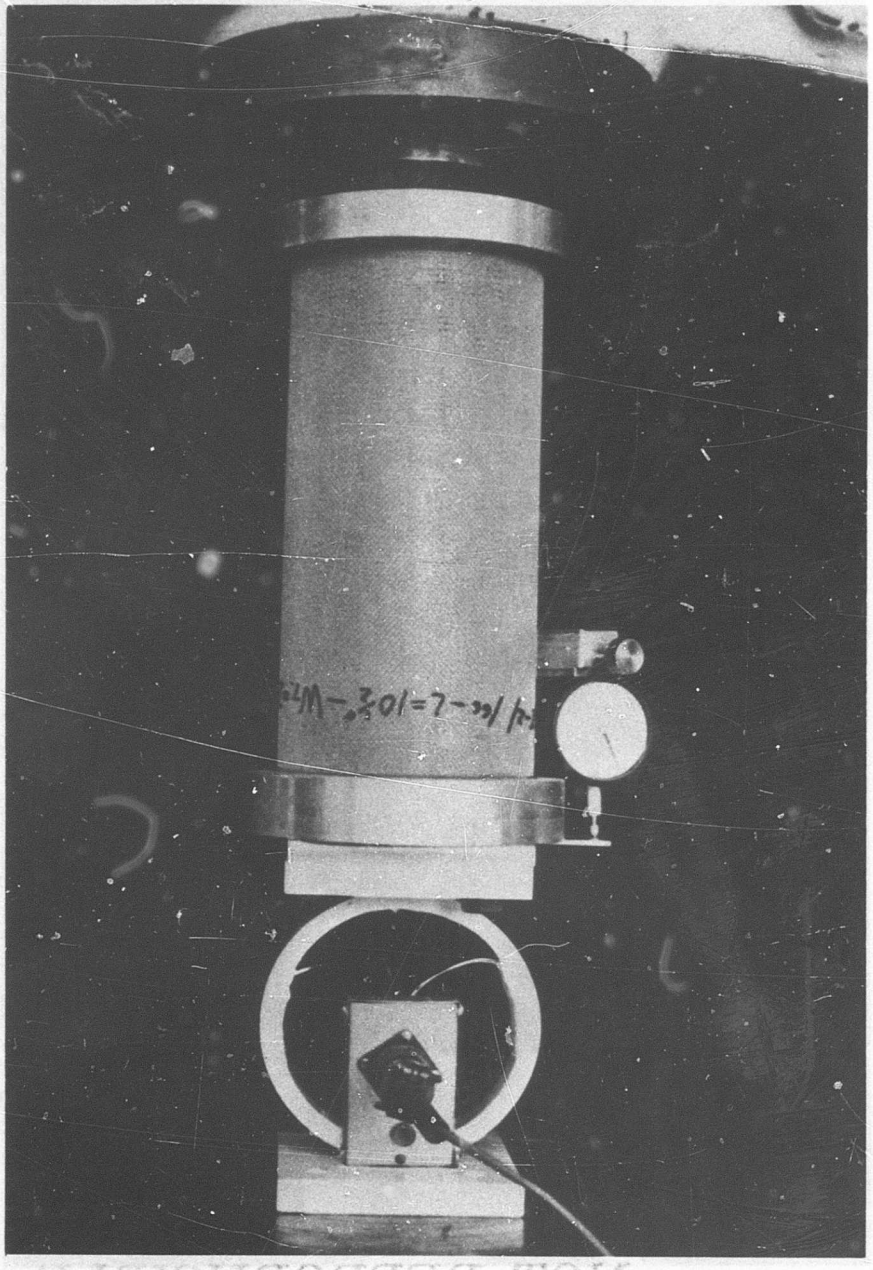

Figure 13. Cylinder in Position for Testing.

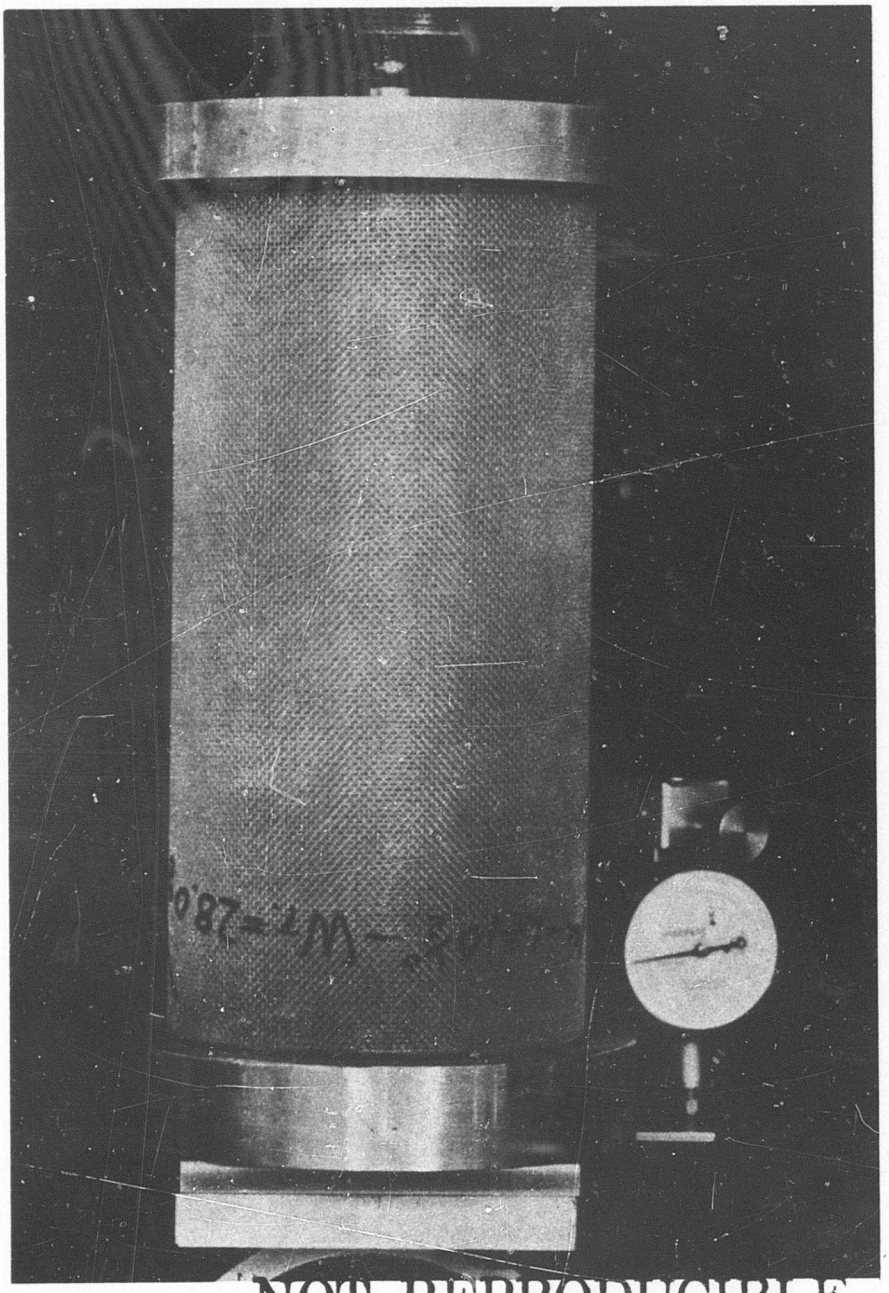

Figure 14. Close-Up of Specimen Prior to Buckling.

DISCUSSION OF RESULTS

The values for the various observations for each cylinder are shown in Table I. The weight and length were obtained as described in the Inspection Procedure section; the end-shortening rate is the slope of the load vs. deflection curve for each specimen. Additional quantities, such as the load-shortening parameter and the total average strain to buckling, were calculated from these values. The calculations were carried out, wherever possible, by means of an automatic digital computer; listings of the programs used are included as Appendix II.

The results were first considered as a whole; then they were broken down into groups having approximately the same layup direction. Four subgroups, representing angles of 0°, 30°, 45°, and 90° to the axis of loading, were so formed. For parameters which appeared to be relatively insensitive to layup angle, the tolerance limits for admission to these subgroups were set rather leniently at $\pm 5^\circ$; this resulted in sample sizes of 23, 27, 24, and 27 specimens, respectively. When the quantity of interest varied considerably with angle, the tolerance limits were reduced to $\pm 2^\circ$, and additional data points were generated at various other angles, for the purpose of comparison, by combining very small groups of specimens or by plotting isolated points.

ADJUSTMENT FOR RESIN CONTENT

Recognized works[12] on the subject of glass fiber-reinforced plastics indicate that considerable variation in strength and modulus is to be expected with variations in the resin-to-glass ratio. To assess this effect, several of the parameters were adjusted by multiplying by various powers of a nondimensional normalizing factor, the ratio of a "nominal weight" of 30.0 grams was in fact not the mean weight of the group, this normalization process had the additional effect of shifting the means of the parameters to which it was applied, as well as of influencing the scatter. However, the effect of significance is the ratio of standard deviation to mean; this gives the best indication of the influence that the normalizing process has on the distribution of the quantity in question.

In the case of the critical buckling load, the distribution is influenced to the best advantage by the second power of the normalizing factor. This is not entirely surprising, in view of the physical significance of that parameter. Analytically, buckling strength is proportional to flexural stiffness, which is proportional to the square of the thickness; for a single layer of reinforced plastic, thickness will be roughly proportional to resin content, which, as mentioned previously, is depicted by the weight of the shell. In any event, the second-power weight adjustment has the effect of altering the distribution of critical load so that it more nearly approximates a normal distribution; this can readily be seen from a comparison of the histograms shown in Figure 15, as well as from the probability plots of Figures 5 and 16 through 18. The ratio of standard deviation to mean is reduced accordingly, as indicated by Table II.

Adjustment for resin content had little effect on the postbuckling load or on the average end shortening per unit length.

TABLE I. CHARACTERISTICS OF SHELLS USED AND RELEVANT TEST DATA

Cylinder No.	Layup Angle, Degree	Weight, g	Length, in.	Critical Load lb.	End Shrt vs. Load lb/in x 10^{-3}	Drop-Off Load lb.	No. of Circumferential Buckles
005	0	32.0	9.50	199	20.95	79.2	7
008	45	27.8	10.00	148	8.86	30.8	6
009	83	29.5	10.44	137	12.62	63.8	6
011	0	27.1	10.25	137	82.50	57.2	6
012	0	27.9	10.31	120	21.92	52.8	6
013	90	28.8	10.25	159	19.68	102.0	6
014	0	27.3	10.38	124	22.36	79.2	6
015	35	27.5	10.31	154	7.35	31.7	7
016	28	29.5	10.12	193	10.91	44.9	6.5
017	78	27.7	10.31	173	16.37	49.7	7
018	32	26.8	10.12	105	6.82	44.0	6.5
020	32	25.9	9.94	124	9.81	47.5	8
021	89	25.4	10.12	130	17.2	60.7	6
022	63	25.6	10.06	120	9.28	53.7	6
023	40	26.4	10.12	110	8.58	39.6	6
024	30	27.2	9.81	156	9.68	40.5	6
025	30	27.5	9.81	136	12.05	44.0	7
026	90	27.6	10.00	167	21.38	66.0	8
027	30	26.4	10.06	138	8.97	44.9	6
028	28	28.8	10.00	175	9.10	39.6	6
029	90	27.6	10.03	164	17.42	64.2	7
030	90	27.2	10.03	127	14.65	-	6
031	29	27.4	9.97	136	8.53	48.4	7
032	32	28.7	9.94	144	6.91	48.4	6
033	0	32.7	9.97	203	28.60	79.1	6
034	90	29.6	10.00	145	20.50	76.1	7
035	0	32.1	10.00	187	25.87	88.0	6
036	0	31.6	10.00	174	16.58	89.0	6
037	90	29.9	9.97	171	15.57	61.6	8
038	0	31.8	9.94	193	26.05	-	6
039	30	29.9	9.97	170	9.59	52.8	7
040	90	26.9	9.97	151	15.22	57.2	8
041	0	26.7	10.00	145	13.28	83.6	8
042	44	28.4	10.00	167	8.45	44.9	6
043	49	28.4	10.06	171	8.27	37.8	6
044	45	30.6	9.97	135	8.23	57.2	6
045	45	29.7	10.00	133	8.84	44.9	7
046	31	31.1	10.00	175	9.02	48.4	6
047	90	30.0	10.00	168	15.13	74.8	8
048	45	28.5	10.03	166	8.31	44.0	6
049	30	27.3	10.00	140	8.22	47.5	7
050	45	28.7	10.03	147	7.04	52.8	7
051	90	26.8	10.00	147	14.39	58.1	8
052	0	26.7	10.03	129	21.56	66.9	7

TABLE I. (Continued)

Cylinder No.	Layup Angle, Degree	Weight, g	Length, in.	Critical Load lb.	End Shrt vs. Load lb/in x 10^{-3}	Drop-Off Load lb.	No. of Circumferential Buckles
053	90	25.8	9.97	127	16.01	66.9	6
054	50	28.9	9.62	153	7.39	46.6	7
055	47	27.8	9.59	133	8.93	42.2	8
056	0	26.8	9.66	141	25.96	66.0	7
057	0	27.8	9.66	132	26.40	72.2	8
058	90	28.4	10.00	148	19.54	70.0	8
059	25	26.9	10.00	149	10.69	44.0	7
060	35	28.4	10.00	145	8.88	44.0	6
061	90	27.0	10.00	162	11.39	58.1	10
062	90	28.1	10.03	161	14.30	66.0	8
063	21	28.5	10.00	183	11.96	46.2	7
064	29	26.9	10.00	153	9.68	41.8	8
065	90	26.3	10.00	163	15.22	54.5	8
066	0	28.0	10.03	172	24.81	64.4	8
067	0	27.2	10.03	166	12.75	46.6	9
068	32	27.9	10.03	151	8.66	44.0	6
069	90	27.9	10.00	151	13.33	59.0	8
070	90	29.7	10.03	142	8.80	75.7	7
071	90	28.3	10.00	160	15.05	75.7	8
072	30	28.6	10.00	194	9.37	52.8	7
073	27	27.3	10.03	170	9.24	55.0	7
074	91	25.3	10.00	120	10.29	60.7	8
075	0	26.0	10.06	150	13.59	52.4	8
076	23	31.1	10.00	172	10.20	52.8	7
077	0	28.0	10.09	167	14.47	52.8	8
078	90	27.2	10.03	169	14.87	75.7	8
079	23	27.6	10.09	165	12.49	53.8	8
080	27	27.2	10.06	169	10.12	48.4	7
081	0	27.5	10.06	116	29.04	-	7
082	48	26.8	10.00	142	7.08	37.8	7
083	52	27.0	10.00	170	8.27	37.4	7
084	90	30.8	10.00	183	9.54	93.4	7
085	90	27.7	10.03	169	17.25	70.9	8
086	92	26.4	10.06	136	19.80	57.2	8
087	27	26.9	10.00	155	11.13	39.6	7
088	90	28.6	10.06	141	17.95	68.2	6
089	27	27.9	10.00	156	11.08	49.3	7
090	30	26.1	10.00	115	8.05	49.3	7
091	90	26.0	10.03	116	10.73	63.8	9
092	43	28.6	10.00	167	9.94	43.1	7
093	45	29.1	10.00	167	8.68	40.5	7
094	90	26.8	10.03	139	12.01	61.6	9
095	49	27.4	9.97	133	7.39	43.1	6
096	30	26.8	10.03	130	8.97	44.0	7

TABLE I. (Continued)

Cylinder No.	Layup Angle, Degree	Weight, g	Length, in.	Critical Load lb.	End Shrt vs. Load lb/in x 10^{-3}	Drop-Off Load lb.	No. of Circumferential Buckles
097	46	28.7	10.00	165	8.22	39.6	6
098	31	27.7	10.09	141	10.03	33.7	6
099	30	26.7	10.03	169	10.47	31.7	7
100	90	26.6	10.00	159	15.44	46.6	8
101	47	28.4	10.09	183	11.49	39.6	6.5
102	47	30.8	9.97	193	11.35	49.3	7
103	46	29.7	10.00	181	9.54	41.8	6
104	0	28.7	10.03	182	28.47	52.8	8
105	0	26.0	10.00	171	27.63	56.3	8
106	45	29.0	10.00	177	9.72	3.87	7
107	0	28.7	10.00	184	30.71	62.5	7
108	40	27.9	9.97	179	11.35	49.3	6
109	30	27.8	9.97	161	13.41	51.9	6
110	0	27.6	9.97	151	26.35	57.2	7
111	47	27.5	9.97	164	9.19	44.9	7
112	0	28.5	10.00	165	13.90	62.5	8
113	46	26.4	10.00	148	9.77	39.6	7
114	47	28.5	10.00	155	11.09	52.8	6.5
115	45	28.1	10.00	166	11.48	48.4	7
116	0	28.4	10.00	167	23.80	71.1	8

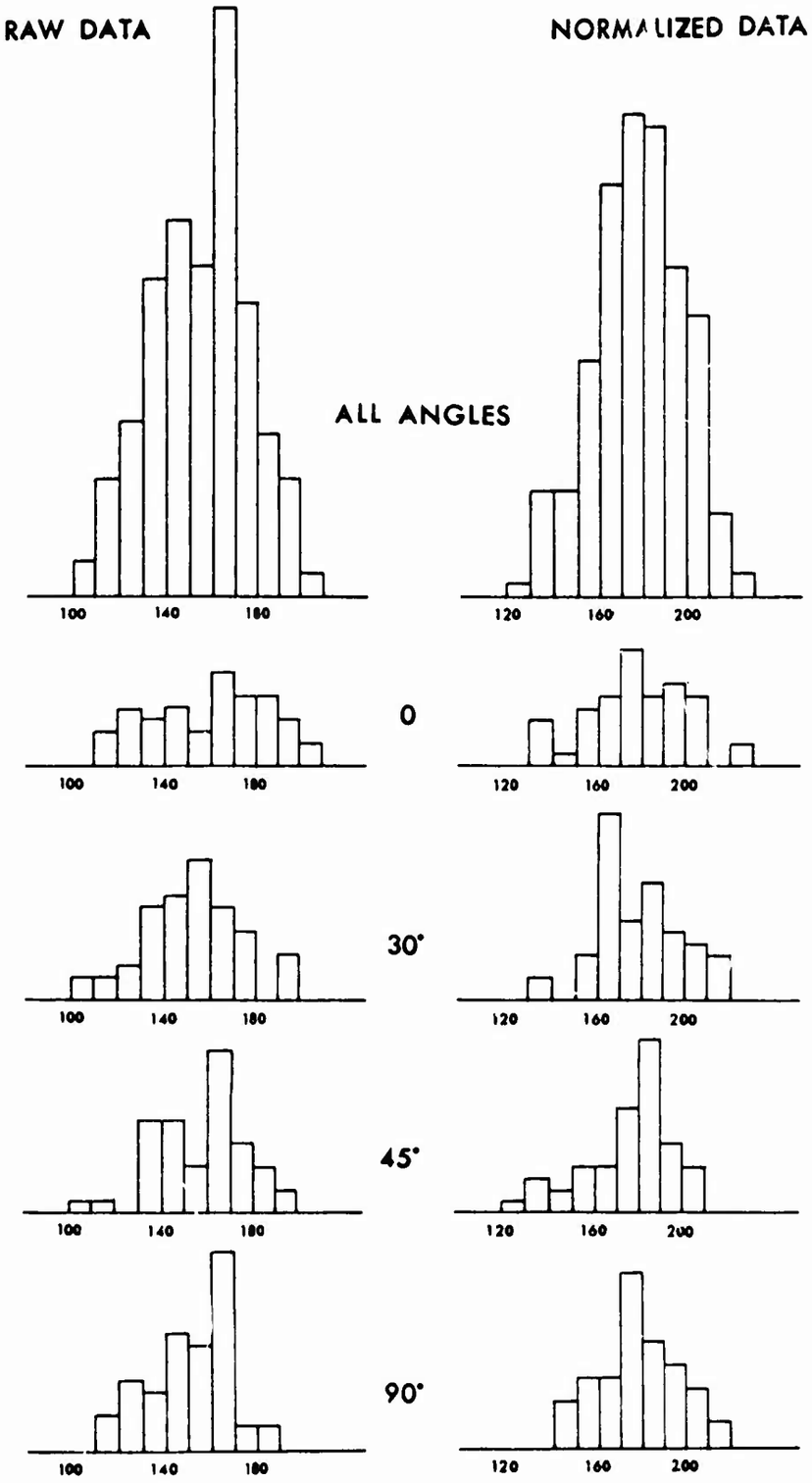

Figure 15. Frequency Distributions of Buckling Loads.

CRITICAL LOADS

The values of buckling load ranged from a high of 203 pounds to a low of 105 pounds. The variability is essentially normal in character, as indicated by the probability plots shown in Figures 16, 17, and 18. This permitted a statistical analysis of the results and the application of the standard significance tests of Reference 15. The means and standard deviations, as well as their ratios for the entire sample and for the various subgroups, are presented in Table II.

Application of the tests outlined in Appendix I leads to the conclusion that the hypothesis that all the means are equal is acceptable at the 5-percent level of significance; moreover, a check on the sensitivity of the test shows a 95-percent probability of detecting a difference in the means of as little as 15-percent, or 22.5 pounds in the case of the raw data. The hypothesis that all the standard deviations are equal is likewise acceptable at the 5-percent level of significance. From this we may conclude, with 95-percent confidence, that the buckling loads for the various subgroups are members of the same population; i.e., that there is no significant difference in critical load due to layup direction.

Consistency between duplicate tests on the same specimen was good. A difference of the order of 5 pounds was the normal. Quite often the second run showed a buckling load equal to or slightly higher than the first, provided damage to the shell was minimized by stopping the test machine motion immediately when buckling occured.

BUCKLING PATTERN

The cylinders invariably buckled in a pattern of diamond-shaped indentations with a wavelength of the order of 2 inches, as shown in Figure 19. In shape, the buckles were somewhat reminiscent of those encountered in Reference 13, except that the elongated lower "tail" of the diamond was seen with less frequency. A similarity to the Yoshimura pattern shown in Reference 14 can be seen. However, the hinge lines at the edges of the buckles were much more rounded than those of either of the two references.

The number of circumferential buckles was determined in a manner similar to that used in Reference 12. However, because of the rounded hinge lines, the delineation of the buckles was somewhat indistinct, and thus the precision of this observation was severely reduced. Accordingly, the values observed were rounded off to the nearest half-buckle, and the results so obtained are usable to indicate a trend only in the most general terms. The median changes from a poorly defined 7 buckles per circumference at 0° to a predominant 8 buckles at 90°.

A helical character to the buckle pattern was also observed, wherein one row would spiral upward slightly, so that upon completion of a revolution it led into the next row above. This phenomenon was observed more frequently in, but was by no means restricted to, the 30° and 45° cylinders.

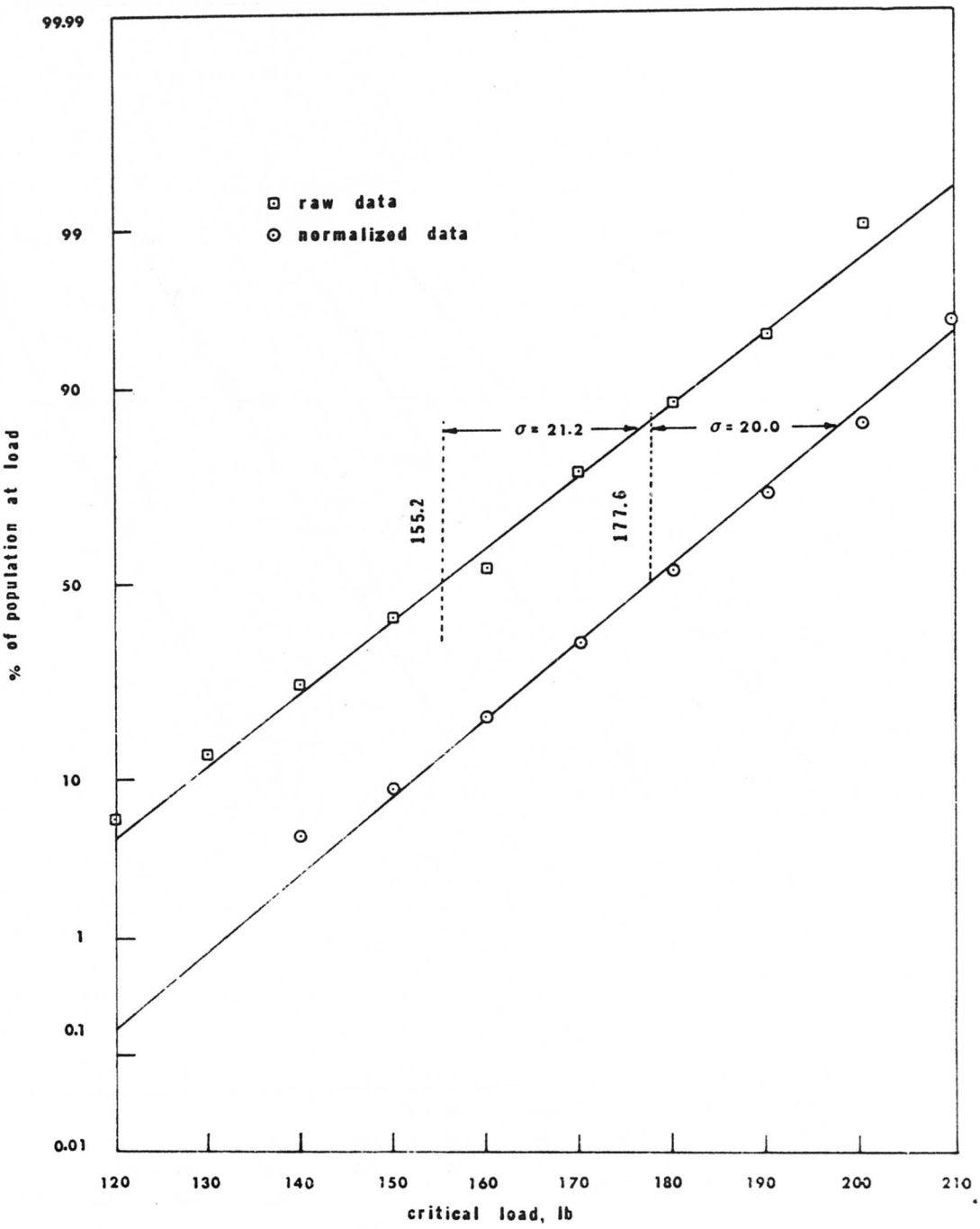

Figure 16. Probability of Plots for Entire Sample of Cylinders.

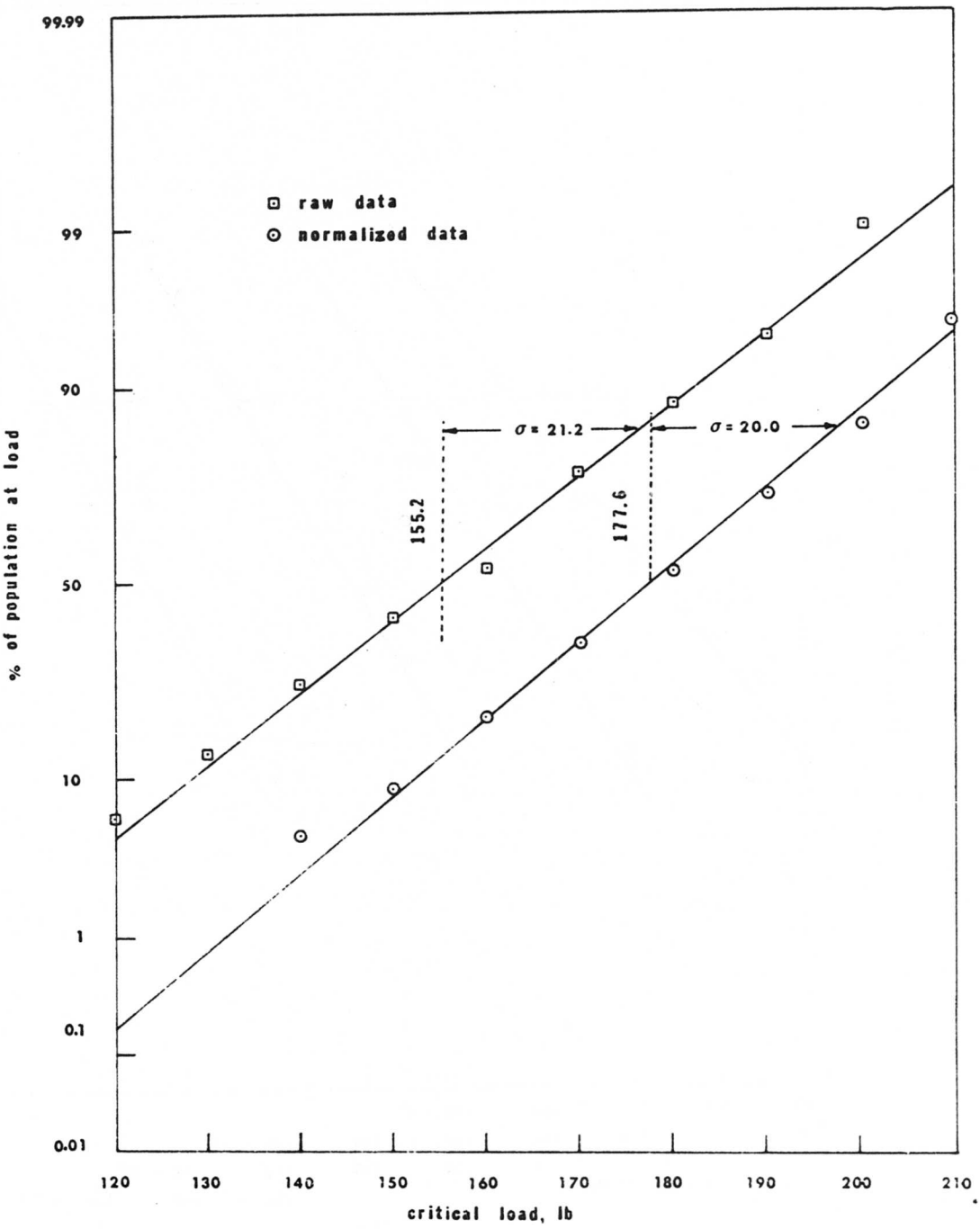

Figure 16. Probability of Plots for Entire Sample of Cylinders.

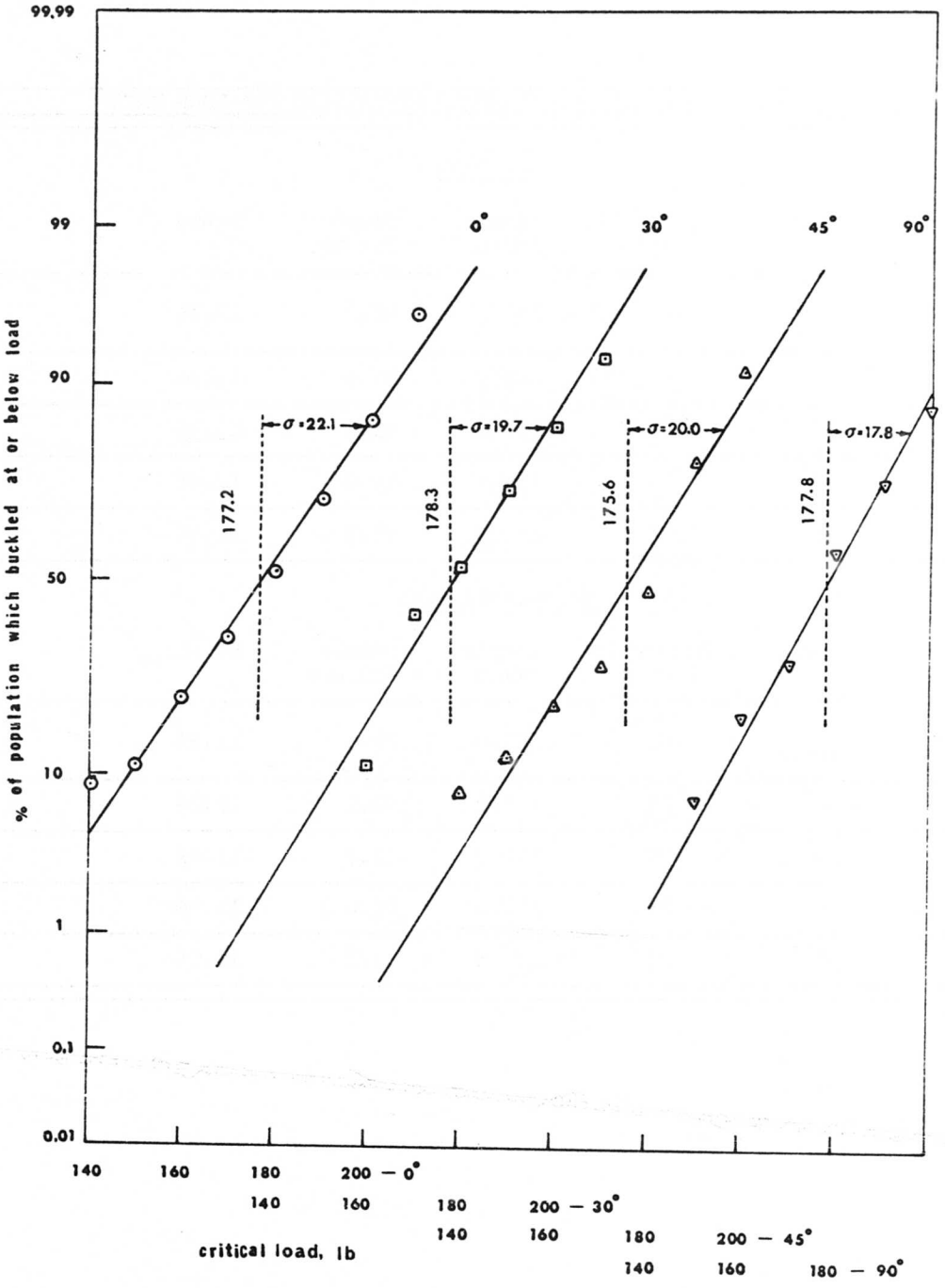

Figure 18. Probability Plots of Normalized Load Data Subdivided by Angle.

TABLE II. SUMMARY OF MEANS AND STANDARD DEVIATIONS FOR LOAD DATA

Raw Data

Angle	Number in Sample	Sample Mean	Sample Std Dev	Ratio
All Angles	108	155.2	21.2	13.7%
0°	23	159.8	25.9	15.2%
30°	27	152.0	21.2	13.9%
45°	24	157.6	19.9	12.6%
90°	27	150.9	17.3	11.5%

Normalized Data

Angle	Number in Sample	Sample Mean	Sample Std Dev	Ratio
All Angles	108	177.6	20.0	11.3%
0°	23	177.2	22.1	12.8%
30°	27	178.3	19.7	11.0%
45°	24	175.6	20.0	11.4%
90°	27	177.8	17.8	10.0%

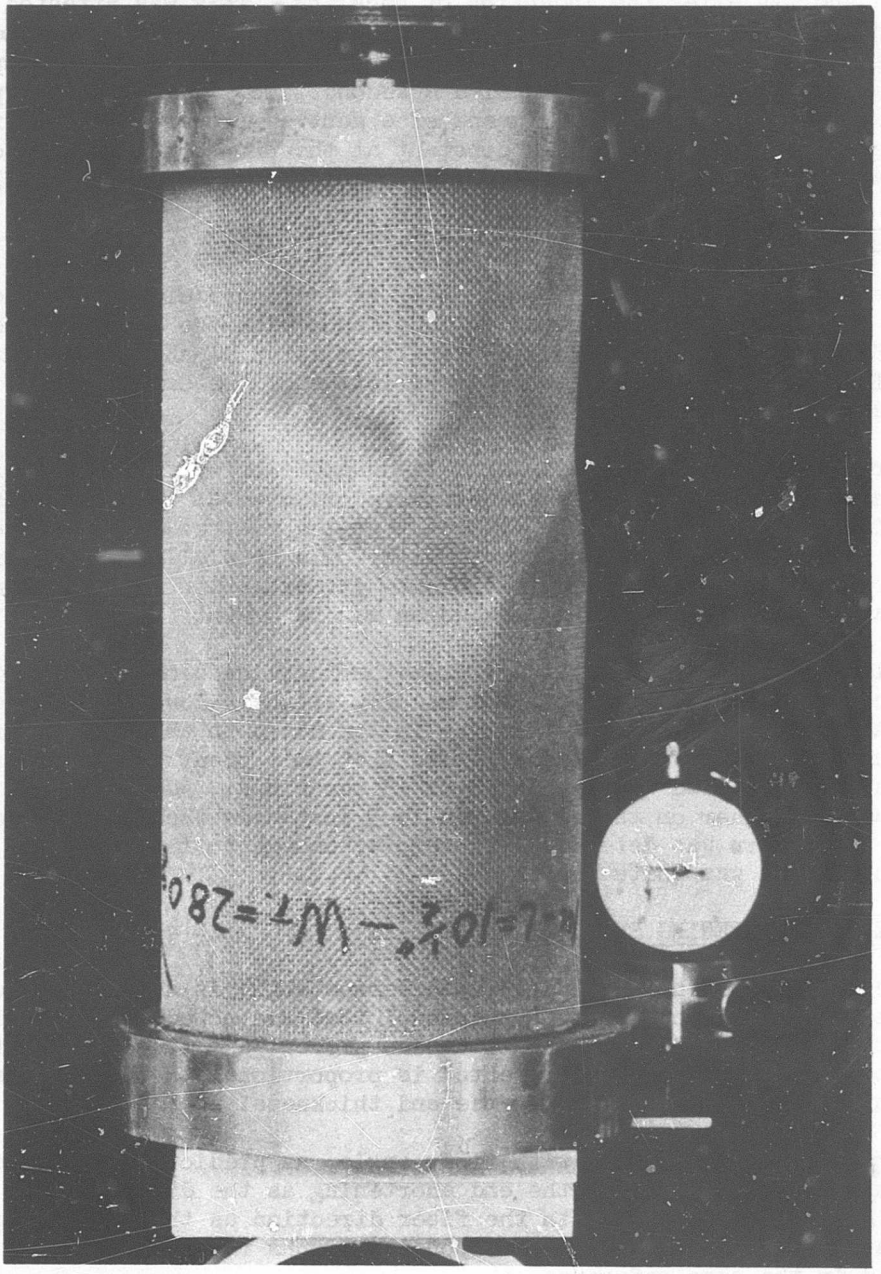

Figure 19. Cylinder After Buckling.

It is considered that the buckles remained elastic, so long as loading was stopped shortly after the inception of buckling. This was attested to by the consistency of the critical loads between runs, as previously mentioned, and also by the fact that 37 of the 108 specimens tested formed completely different pattern upon being buckled a second time. Moreover, the patterns were easily interchangeable by means of a gentle pressure on the surface of the shell, as the load was held constant at the drop-off value. A cylinder with two successive patterns indicated thereon is shown in Figure 21.

POSTBUCKLING LOAD

The postbuckling load, or falloff load, varied considerably with layup angle. It was therefore treated in accordance with the procedure described above for such parameters, and the resulting curve is shown in Figure 20. Table III presents a more detailed description of the origin of the points plotted in the figure.

The curve shows a minimum load for a layup angle of 45°. From the fact that the hinge lines of the buckle pattern were oriented at an angle near 45° (see Figure 19), it may be conjectured that the postbuckling load is influenced by the flexibility of these hinges, which would naturally be greater in a direction parallel to the fibers. Much more investigation of this phenomenon is necessary before any definite conclusion can be drawn.

Some slight damage to the cylinder from the buckling process was indicated by the fact that the drop-off load was usually slightly lower on the second run. A notable exception to this was in the cases in which a different pattern was manifest. For the 37 times that this occurred, a higher second-run postbuckling load was developed on 13 occasions. Additionally, the fall-off load was higher on the second run in 3 instances where no appreciable change in pattern was detected. Therefore, damage to the specimens was present, but it was quite small.

AVERAGE END SHORTENING PER UNIT LENGTH

Average end shortening per unit length versus angle is shown in Figure 22a, and the various sources for the points plotted are noted in Table III. The impracticability of determining thickness prevented a true modulus from being presented, but the variable presented is proportional to the modulus, on the assumption of constant circumference and thickness.

The parameter varies widely with fiber angle, as predicted in Reference 12. In fact, a polar plot, with the end shortening as the distance from the origin along a radius and with the fiber direction as the angle (Figure 22b), bears a great resemblance to corresponding graphs for bidirectional fabrics depicted in the same reference.

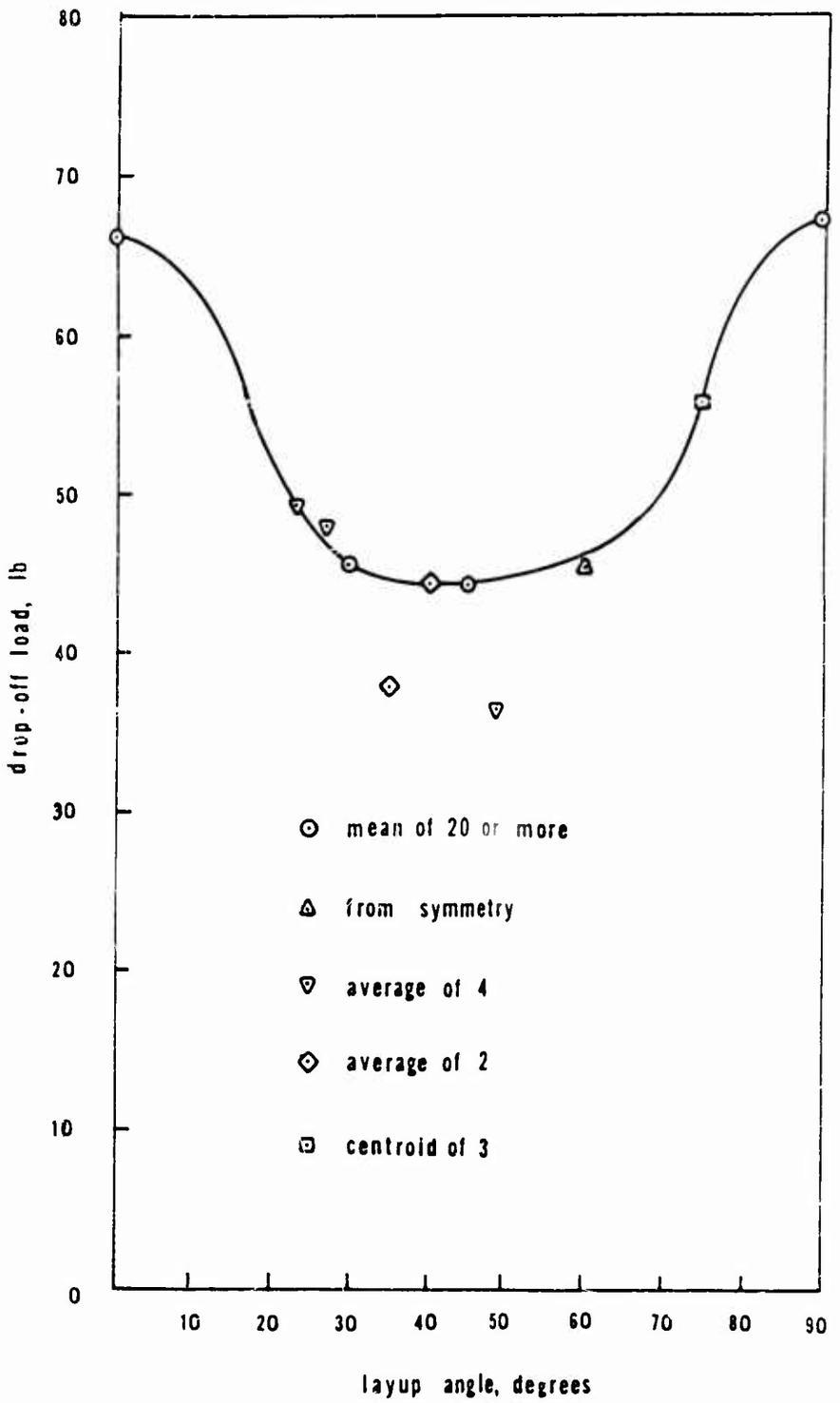

Figure 20. Plot of Postbuckling Load versus Fiber Direction.

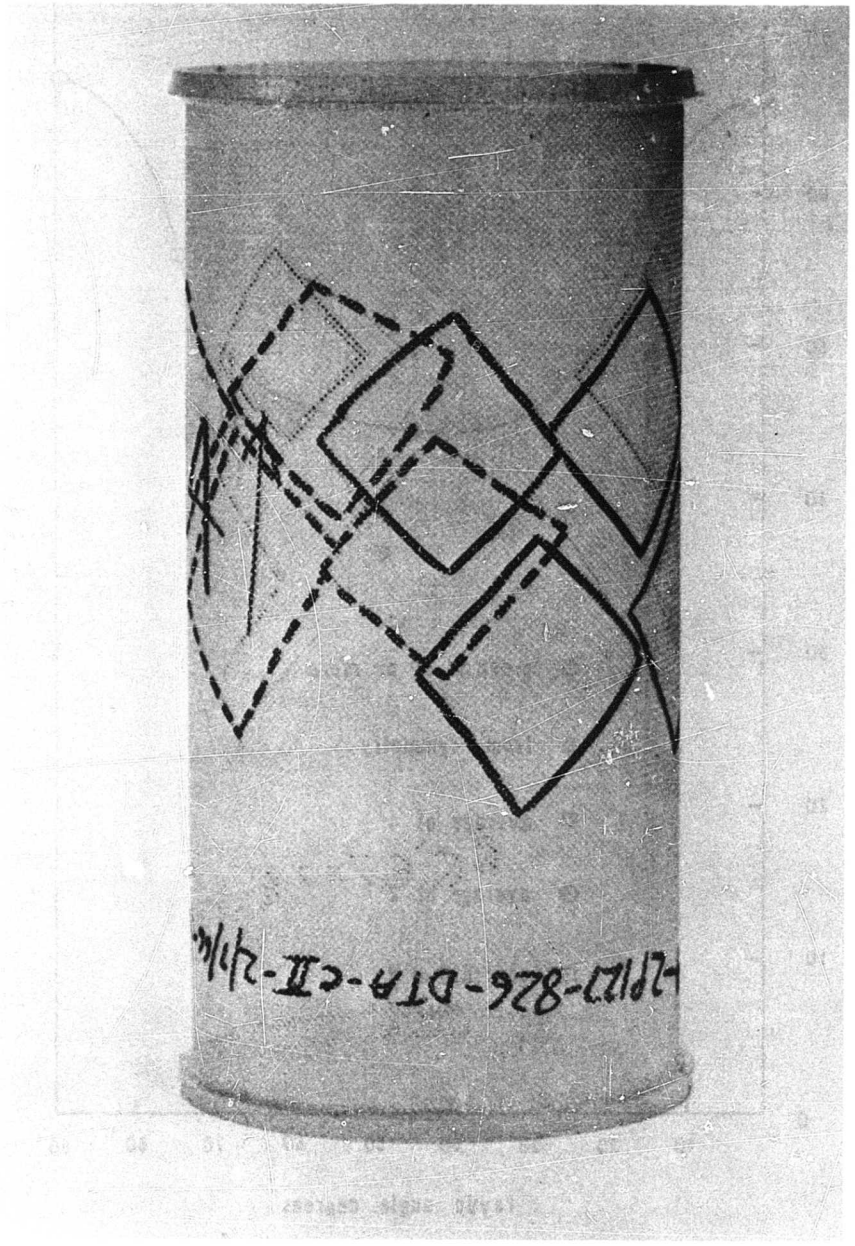

Figure 21. Cylinder Showing Two Distinct Buckle Patterns.

TABLE III. DATA POINTS FOR PARAMETERS WHICH VARY WIDELY WITH ANGLE

Angle, Deg	Fall Off Load, lb	Load-Strain Parameter $lb \times 10^{-3}$	Remarks
0	$\bar{x} = 66.3$ $s = 12.8$	$\bar{x} = 224.6$ $s = 58.0$	n = 21, 22, respectively
23	49.2	112.6	average of 4
27	48.1	104.1	average of 4
30	$\bar{x} = 45.5$ $s = 3.8$	$\bar{x} = 94.0$ $s = 15.2$	n = 20
35	37.8	82.3	average of 2
40	44.4	100.0	average of 2
45	$\bar{x} = 44.2$ $s = 6.1$	$\bar{x} = 92.7$ $s = 14.2$	n = 18
49	41.3	74.7	average of 4
60	45.5	94.0	by symmetry
75	55.7	140.0	centroid of 3
90	$\bar{x} = 67.2$ $s = 11.7$	$\bar{x} = 153.2$ $s = 34.0$	n = 26, 27, respectively

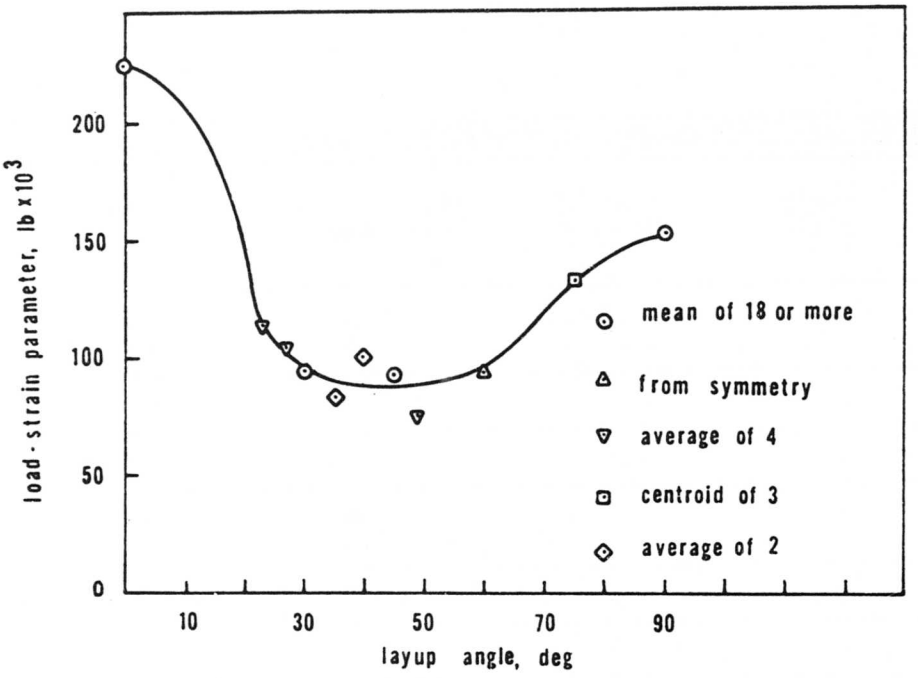

a. Cartesian Coordinates

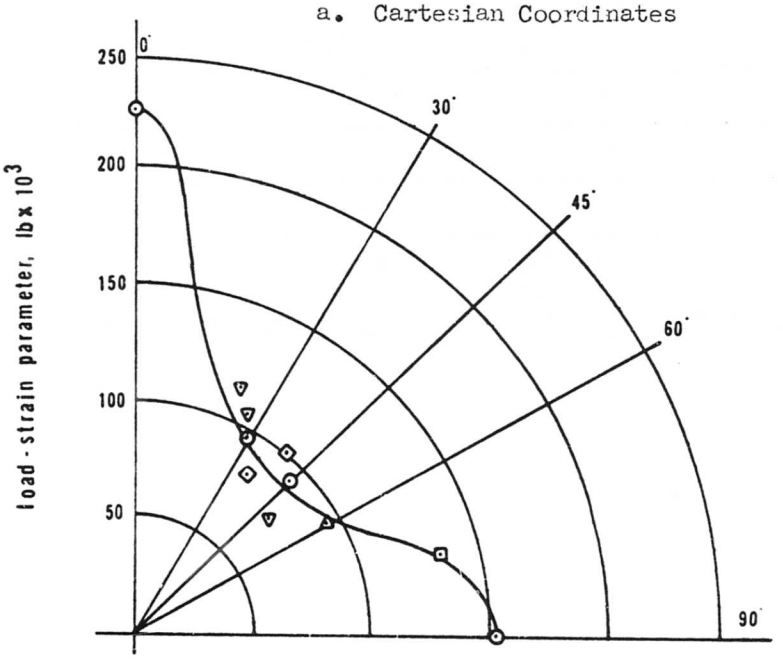

b. Polar Coordinates

Figure 22. Plots of Load-Strain Parameter vs. Fiber Direction.

ADDITIONAL CONFIRMATORY TESTS

To check whether the results of the previous tests were a direct consequence of the open-weave structure, additional tests were made. The specimens for these supplementary tests were right-circular cylinders of approximately the same geometry, diameter and length, as those used in the main investigation. However, these specimens were made from 181 glass-cloth, a material of much denser weave than 2P127 cloth. The type of glass and finish, the resin system used, and the cure cycle carried out were all identical to those previously used. However, the seaming process was significantly different. The 181-fabric specimens were seamed on an internal mandrel by much the same method as was used in Reference 13, except that instead of a soldered lap joint, a butt joint was used with a 5/8-inch-wide lapping strip of 2P127-fabric fastened in place with epoxy. This technique afforded extremely good dimensional control of the specimens: in addition, it provided a convenient method of handling the somewhat intractable 181-fabric layup. The adhesive, a mixture of 100 parts Epon 826 with 24 parts Hardener T-1, was applied by means of a conventional hobby shop "glue gun", as shown in Figure 23. This application was carried out with the entire assembly raised to 175 F, a temperature above the heat-distortion level of the cylinder's resin system, thus relieving any internal stresses which might have been introduced by the process. The elevated temperature also provided sufficient clearance to permit removal of the specimen from the mandrel after cooling.

Two specimens of this type were fabricated and tested, one with a layup direction parallel to the load direction and one at 45° to the load direction. The results are presented in Table IV. These observations are in substantial agreement with those obtained for the open-weave cylinders.

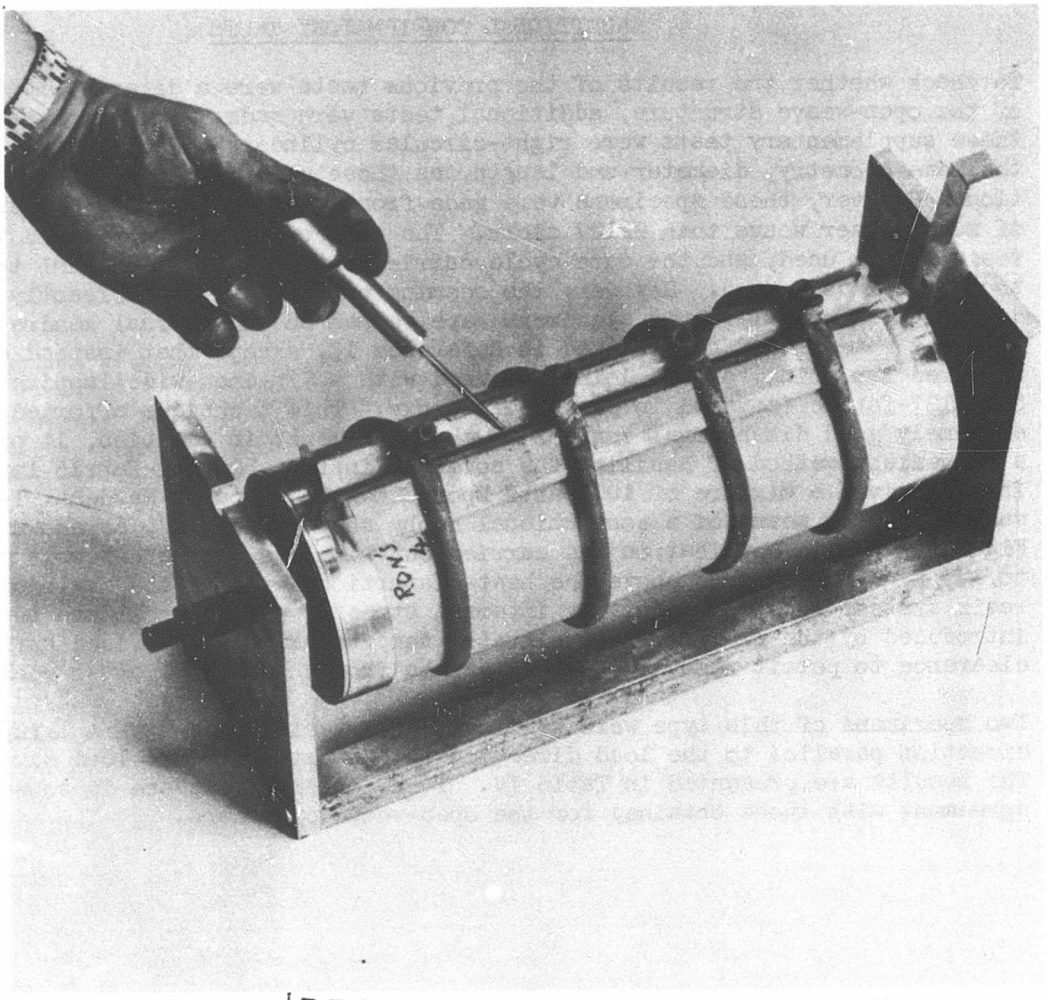

Figure 23. Seaming Process for 181-Fabric Cylinders.

TABLE IV. RESULTS OF ADDITIONAL CONFIRMATORY TESTS, USING CYLINDERS OF 181-FABRIC LAMINATE

Nominal Angle, Deg	Run	Critical Load, lb	Falloff Load, lb
0	1	568	181
	2	480	180
	3	458	179
45	1	559	118
	2	552	115
	3	550	114

CONCLUSIONS

The experiments reported herein demonstrate that fiber direction, while of extreme importance in questions of strength or stiffness, does not materially influence the initial critical loads for instability in single-layer glass-cloth resin-impregnated shells. Furthermore, the work shows that the effect of repeated loading is dependent upon fiber direction. This fact is associated with the increasing damage experienced by fibers as their direction becomes more skew to the fold lines.

REFERENCES

1. Nash, W. A., BIBLIOGRAPHY ON SHELLS AND SHELL-LIKE STRUCTURES, University of Florida, Contract DA-01009-ORD-404, U. S. Army, Office of Ordnance Research, 1957.

2. Nash, W. A., BIBLIOGRAPHY ON SHELLS AND SHELL-LIKE STRUCTURES, TBM Report 863, U. S. Navy Department, David Taylor Model Basin, Washington, D. C., 1954.

3. Hoff, N. J., BUCKLING OF THIN SHELLS, Proceedings of an Aerospace Symposium of Distinguished Lectures in Honor of Dr. Theodore von Kármán on His 80th Anniversary, May 11, 1961, The Institute of Aerospace Sciences, New York, p. 1.

4. Fung, Y. C., and Sechler, E. E., INSTABILITY OF THIN ELASTIC SHELLS, Proceedings of the First Symposium on Naval Structural Mechanics, Pergamon Press, 1960, pp. 115-168.

5. Lee, L. H. N., EFFECTS OF MODES OF INITIAL IMPERFECTIONS ON THE STABILITY OF CYLINDRICAL SHELLS UNDER AXIAL COMPRESSION, NASA TN D-1510, December 1962.

6. Horton, W. H., THE PHILOSOPHY OF EXPERIMENTAL RESEARCH, SUDAER No. 229, Stanford University, November 1965.

7. Horton, W. H., and Cox, J. W., THE STABILITY OF THIN-WALLED UNSTIFFENED CIRCULAR CYLINDRICAL SHELLS UNDER NONUNIFORMLY DISTRIBUTED AXIAL LOAD, SUDAER No. 220, Stanford University, February 1965.

8. Union Carbide Corporation, STRONGEST MATERIAL FOR ITS WEIGHT EVER PRODUCED ANNOUNCED BY UNION CARBIDE, published in Carbon Products News.

9. Hackman, L. E., Stotler, C. L., Worthington, D. G., and Molella, R. J., STRUCTURAL FIBER GLASS AIRCRAFT COMPONENT-PROGRAM RESULTS, Journal of Aircraft, Vol. 2, No. 3, May-June 1965, pp. 216-223.

10. Cheng, S., and Ho, B. P. C., STABILITY OF HETEROGENEOUS AEOLOTROPIC CYLINDRICAL SHELLS UNDER COMBINED LOADING, AIAA Journal, Vol. 1, No. 4, April 1963, pp. 892-898.

11. Ho, B. P. C., and Cheng, S., SOME PROBLEMS IN STABILITY OF HETEROGENEOUS AEOLOTROPIC CYLINDRICAL SHELLS UNDER COMBINED LOADING, AIAA Journal, Vol. 1, No. 7, July 1963, pp. 1603-1607.

12. MIL-Handbook-17, PLASTICS FOR FLIGHT VEHICLES - PART I, Reinforced Plastics, Chapter 2, as revised May 1, 1964.

13. Komp, R. L., THE INFLUENCE OF GEOMETRY ON THE BUCKLING OF THIN-WALLED CIRCULAR CYLINDRICAL SHELLS, Engineer's Thesis, Stanford University, July 1965.

14. Edwards, A. M., THE EFFECTS OF PLASTICITY ON THE BUCKLING AND POST-BUCKLING OF CIRCULAR CYLINDRICAL SHELLS, Ph.D. Thesis, Stanford University, June 1965.

15. Bowker, A. H., and Lieberman, G. J., ENGINEERING STATISTICS, Prentice-Hall, Inc., 1959.

APPENDIX I
STATISTICAL TREATMENT OF BUCKLING LOAD RESULTS

The procedures followed are standard significance tests such as are described in most modern references on experimental statistics, notably that by Bowker and Lieberman.[15] The mean of each of the subgroups was compared with the grand mean and with that of every other subgroup by methods based upon Student's "t" distribution. These were preferred to an Analysis of Variance technique because of their relative simplicity and their greater ability to evaluate Errors of the Second Kind. A confidence level of 95-percent was required in all tests utilized here. Relevant data are presented in Table II.

To compare the individual means ($\bar{x}$) with the grand mean (μ_o), the test statistic

$$t = (\bar{x} - \mu_o)\sqrt{n}/s \tag{1}$$

was calculated on a digital computer (see Appendix II) for each subgroup. The results so obtained are shown in Table V. The rejection criterion for the two-sided alternative is

$$|t| \geq t_{\alpha/2;\ n-1} \tag{2}$$

the 100 $\alpha/2$ percentage point of the t distribution with n - 1 degrees of freedom ($\alpha/2 = 0.025$ at the 95-percent confidence level). From tables of the t distribution,

$$t_{.025;\ 22} = 2.074$$

$$t_{.025;\ 23} = 2.069 \tag{3}$$

and

$$t_{.025;\ 26} = 2.056$$

Hence, none of the hypothesis that $\mu - \mu_o$ should be rejected at the $\alpha = .05$ level of significance.

The risk of an Error of the Second Kind is evaluated by means of the relevant Operating Characteristic Curve, presented in Figure 6.10 of Reference 15. Entering this curve with $\beta = .05$ and $n \cong 25$, we obtain

$$d = (\mu - \mu_o)/\sigma = 0.8 \tag{4}$$

A calculation of the type

$$\text{detectable error} = \frac{(\mu-\mu_o)}{\mu_o} = \frac{d\sigma}{\mu_o} \cong \frac{0.8 \times s}{\mu_o} \tag{5}$$

shows the detectable error to be of the order of 10-percent for the raw data

TABLE V. VALUES OF TEST STATISTICS IN ACCORDANCE WITH EQUATION 1

Angle (deg)	n	t Statistic for Raw Data	t Statistic for Normalized Data
0	23	0.86	0.09
30	27	0.77	0.17
45	24	0.61	0.49
90	27	1.27	0.06

TABLE VI. VALUES OF TEST STATISTICS IN ACCORDANCE WITH EQUATION 7

	Raw Data			Normalized Data		
Angle (deg)	30°	45°	90°	30°	45°	90°
0	1.17	0.34	1.44	0.18	0.26	0.11
30	-	0.97	0.20	-	0.47	0.09
45	-	-	1.29	-	-	0.41

and 9-percent for the normalized data.

The two-parameter t-test, used to compare the subgroup means to each other, while allowing the standard deviations to be unknown, requires the assumption that they be equal to one another. This is quite reasonable on the basis of an a priori look at the data (see Table II); however, a further check was carried out, using Cochran's test for the Homogeneity of Variances. The test statistic

$$g = \frac{\text{largest } s^2}{s_1^2 + s_2^2 + \cdots s_k^2} \tag{6}$$

is evaluated as $g = 0.37$ for the raw data and as $g = 0.31$ for the normalized data. The rejection criterion is $g > g_\alpha$ has been suitably chosen for sample size n and number of variances K. Table 7.8 of Reference 15 evaluates g at 0.41 for $\alpha = .05$. Therefore, the hypothesis of equality of variances is accepted, and the analysis of the means may then proceed.

For every pair of means, the test statistic

$$t = (\bar{x} - \bar{y})\left(\frac{1}{n_x} + \frac{1}{n_y}\right)^{-\frac{1}{2}} \left[\frac{\left(\sum (x_i - \bar{x})^2 + \sum (y_i - \bar{y})^2\right)}{(n_x + n_y - 2)}\right]^{-\frac{1}{2}} \tag{7}$$

was evaluated on the computer, with the results given in Table VI. The rejection criterion is

$$| t | \geq t_{\alpha/2;n_x + n_y - 2} \cong 2.01 \tag{8}$$

Again, all hypotheses are accepted at the $\alpha = .05$ level of significance.

A check on the Error of the Second Kind, corresponding to that performed above, shows the detectable error to be of the order of 15-percent for both raw and normalized data.

APPENDIX II
LISTINGS OF ALGOL PROGRAMS USED IN DATA REDUCTION ON BURROUGHS B-5500 DIGITAL COMPUTER

```
BEGIN
   COMMENT ACCEPTS DATA CARDS WITH CYLINDER NUMBER, LAYUP ANGLE, WEIGHT,
      MOUNTED LENGTH, CRITICAL LOAD, AND SLOPE OF LOAD-DEFLECTION CURVE;
   COMMENT OUTPUTS FOR EACH CYLINDER VALUES OF CRITICAL BUCKLING LOAD,
      LOAD-STRAIN PARAMETER, AND TOTAL AVERAGE STRAIN TO FAILURE, PLUS
      FIRST, SECOND, THIRD, AND FOURTH-POWER NORMALIZATIONS OF EACH;
   COMMENT ADDITIONAL OUTPUT IS SUM AND SUM OF SQUARES FOR EACH
      PARAMETER;

   INTEGER NUM, ANG, L0, L1, L2, L3, L4, SL0, SL1, SL2, SL3, SL4, SSL0,
      SSL1, SSL2, SSL3, SSL4;
   REAL W1, LN, RM, M0, M1, M2, M3, M4, LD1, LD2, LD3, LD4, E0, E1, E2,
      L3, E4, SM0, SM2, SM3, SM4, SSM0, SSM1, SSM2, SSM3, SSM4,
      SE0, SE1, SE2, SE3, SE4, SSE0, SSE1, SSE2, SSE3, SSE4, LD0;
   LABEL INGRESS, EXIT;
   FORMAT FMT("CYL NUMBER", I6, X10, "ANGLE", I5, X4, "WEIGHT", F8.1);

   PROCEDURE NORMALIZE(X, WT)"RESULT:"(X1, X2, X3, X4);
      REAL X, WT, X1, X2, X3, X4;
   BEGIN
      X1←((30 x X)/WT);
      X2←((900 x X)/(WT x WT));
      X3←((27000 x X)/(W1 x WT x WT));
      X4←((810000 x X)/(WT x WT x WT x WT));
   END NORMALIZE;

   SL0←SL1←SL2←SL3←SL4←SSL0←SSL1←SSL2←SSL3←SSL4←0;
   SM0←SM1←SM2←SM3←SM4←SSM0←SSM1←SSM2←SSM3←SSM4←0;
   SE0←SE1←SE2←SE3←SE4←SSE0←SSE1←SSE2←SSE3←SSE4←0;

INGRESS:  READ(NUM, ANG, WT. LN, LD0, RM)[EXIT];
   M0←(RM x LN);
   E0←(LD0/M0);

   NORMALIZE(LD0, WT, LD1, LD2, LD3, LD4);
      L0←ENTIER(LD0 + 0.5);      SL0←SL0 + L0;      SSL0←SSL0 + (L0 x L0);
      L1←ENTIER(LD1 + 0.5);      SL1←SL1 + L1;      SSL1←SSL1 + (L1 x L1);
      L2←ENTIER(LD2 + 0.5);      SL2←SL2 + L2;      SSL2←SSL2 + (L2 x L2);
      L3←ENTIER(LD3 + 0.5);      SL3←SL3 + L3;      SSL3←SSL3 + (L3 x L3);
      L4←ENTIER(LD4 + 0.5);      SL4←SL4 + L4;      SSL4←SSL4 + (L4 x L4);

   NORMALIZE(M0, WT, M1, M2, M3, M4);
      SM0←SM0 + M0;      SSM0←SSM0 + (M0 x M0);
      SM1←SM1 + M1;      SSM1←SSM1 + (M1 x M1);
      SM2←SM2 + M2;      SSM2←SSM2 + (M2 x M2);
      SM3←SM3 + M3;      SSM3←SSM3 + (M3 x M3);
      SM4←SM4 + M4;      SSM4←SSM4 + (M4 x M4);
```

```
    NORMALIZE(E0, WT, E1, E2, E3, E4);
       SE0←SE0 + E0;      SSE0←SSE0 + (E0 x E0);
       SE1←SE1 + E1;      SSE1←SSE1 + (E1 x E1);
       SE2←SE2 + E2;      SSE2←SSE2 + (E2 x E2);
       SE3←SE3 + E3;      SSE3←SSE3 + (E3 x E3);
       SE4←SE4 + E4;      SSE4←SSE4 + (E4 x E4);

    WRITE([DBL]);      WRITE([DBL]);
    WRITE([DBL], FM1, NUM, ANG, WT);
    WRITE([DBL],<X10, "LOAD", X6,5I20>,L0, L1, L2, L3, L4);
    WRITE([DBL], <X10,"MODULUS", X3, 5F20.10>, M0, M1, M2, M3, M4);
    WRITE(<X10, "STRAIN", X4, 5F20.10>, E0, E1, E2, E3, E4);

 GO TO INGRESS;

 EXIT:  WRITE([PAGE]);
    WRITE([DBL], <"SUMS">);
    WRITE([DBL], <"LOAD",X16, 5I20>, SL0, SL1, SL2, SL3, SL4);
    WRITE([DBL], <"MODULUS", X13, 5F20.4>, SM0, SM1, SM2, SM3, SM4);
    WRITE([DBL], <"STRAIN", X14, 5F20.4>, SE0, SE1, SE2, SE3, SE4);
    WRITE([DBL]);      WRITE([DBL]);
    WRITE([DBL], <"SUMS OF SQUARES">);
    WRITE([DBL], <"LOAD", X16, 5I20>, SSL0, SSL1, SSL2, SSL3, SSL4);
    WRITE(<"MODULUS", X13, 5F20.4>, SSM0, SSM1, SSM2, SSM3, SSM4);
    WRITE([DBL]);
    WRITE([DBL], <"STRAIN", X14, 5F20.4>, SSE0, SSE1, SSE2, SSE3, SSE4);
 END.
?32                  PRECEDES B5000 AND I8JOB DATA CARDS
```

```
BEGIN
   COMMENT ACCEPTS N SUMS, SUMS OF SQUARES, AND SAMPLE SIZES PLUS GRAND
      SUM AND SAMPLE SIZE, AND CALCULATES ONE-PARAMETER STUDENTS "T"
      BETWEEN EACH MEAN AND GRAND MEAN, PLUS TWO-PARAMETER STUDENTS "T"
      BETWEEN EACH MEAN AND EVERY OTHER;

   INTEGER N;
   READ(N);
   BEGIN COMMENT INNER BLOCK STARTS HERE;
      INTEGER I, SIGN, J, K, L, M, P, Q;
      REAL MUZERO, BIGSUM;
      REAL ARRAY SUM, SUMSQ, TONE[1:N], [TWO[1:N,1:N];
      INTEGER ARRAY NUM[1:N];
      FORMAT FMT(4F20.10);

   REAL PROCEDURE TEEDNE(SUM, SUMSQ, EN, MUZERO);
      REAL SUM, SUMSQ, MUZERO;
      INTEGER EN;
      BEGIN
         REAL VAR, XBAR;
         VAR←SQRT((SUMSQ-(SUMxSUM/EN))/(EN-1));
         XBAR←SUM/EN;
         TEEDNE←(ABS(XBAR-MUZERO)}x(SQRT(EN))/VAR;
      END TEEDNE;
   REAL PROCEDURE TEETWO(SUMX, SUMY, SUMSQZ, SUMSQY, NX, NY);
      REAL SUMX, SUMY, SUMSQX, SUMSQY;
      INTEGER NX, NY;
      BEGIN
         REAL TEMP, MEANDIF;
         TEMP←(SUMSQX - (SUMX x SUMX / NX) + SUMSQY - (SUMY x SUMY / NY));
         MEANDIF←ABS((SUMX / NX) - (SUMY / NY));
         TEETWO←MEANDIFxSQRT((NXxNYx(NX+NY-2))/((NX+NY)xTEMP));
      END TEETWO;

      FOR I←1 STEP 1 UNTIL N DO READ(SUM[I], SUMSQ[I], NUM[I]);
      READ(BIGSUM, BIGN);
      MUZERO←BIGSUM/BIGN;

      COMMENT NEXT STEPS FILL MATRICES WITH STUDENTS T VALUES;
      FOR J←1 STEP 1 UNTIL N DO
         TONE[J]←TEEDNE(SUM[J], SUMSQ[J], NUM[J], MUZERO);
      FOR K←1 STEP 1 UNTIL N DO
         FOR L←1 STEP 1 UNTIL N DO
            TTWO[K,L]←TEETWO(SUM[K], SUM[L], SUMSQ[K], SUMSQ[L], NUM[K],
                                                                 NUM[L];
      WRITE(<"COMPARISON OF INDIVIDUAL MEANS WITH OVERALL MEAN">);
      WRITE([DBL]);
      WRITE(FMT, FOR M←1 STEP 1 UNTIL N D) TONE[M]);
      WRITE([PAGE]);
      WRITE(<"COMPARISON OF INDIVIDUAL MEANS WITH EACH OTHER">);
```

```
    WRITE([DBL]);
    FOR P←1 STEP 1 UNTIL N DO BEGIN
       WRITE([DBL]);
       WRITE(FMT, FOR Q←1 STEP 1 UNTIL N DO TTWO[P,Q]);
    END;
END INNER BLOCK;
END.
?32                 PRECEDES B5000 and IBJOB DATA CARDS
```